MÉTÉO-FRANCE-CNRS/CNRM
CEN (SNOW RESEARCH CENTRE)

MASTER THESIS

Synthesis of distributed snowpack simulations relevant for avalanche hazard forecasting

Author:
Coline BOUCHAYER

Supervisors:
Dr. Vincent VIONNET
and Dr. Pascal HAGENMULLER

A thesis submitted in fulfillment of the requirements for the degree of Master of Science

in the

University Grenoble Alpes/UniLasalle
Master of Science-Atmosphere, Climate, Continental Surfaces

Declaration of Authorship

Je soussignée, Coline BOUCHAYER, auteur du mémoire, "Synthesis of distributed snowpack simulations relevant for avalanche hazard forecasting",
Déclare sur l'honneur que ce mémoire est le fruit d'un travail personnel et que je n'ai ni contrefait, ni falsifié, ni copié tout ou partie de l'œuvre d'autrui afin de la faire passer pour la mienne. Toutes les sources d'information utilisées et les citations d'auteur ont été mentionnées conformément aux usages en vigueur. Je suis consciente que le fait de ne pas citer une source ou de ne pas la citer clairement et complètement est constitutif de plagiat, et que le plagiat est considéré comme une faute grave au sein de l'Université, pouvant être sévèrement sanctionnée par la loi.

Fait à : Grenoble
Date: 16/06/2017
Signature de l'étudiante:

Abstract

[English] Numerical weather prediction (NWP) systems operating at kilometer scale in mountainous terrain offer appealing prospects for forecasting the state of the snowpack in support of avalanche hazard warning. In this study, daily forecasts of the NWP system Applications of Research to Operations at Mesoscale (AROME) at 1.3-km grid spacing over the French Alps were considered to provide atmospheric forcing to the snowpack model Crocus. No effect of orientations and slopes neither wind-induced snow transport are taken into account. These simulations produce a huge amount of data that needs to be synthesized into reduced but relevant information that captures the spatial variability of the snowpack, which is critical for the avalanche risk forecasting. The present study uses statistical approaches such as the Principal Component Analysis (PCA) and clustering techniques to characterise the snowpack spatial variability at the massif scale and focuses on two controlling ingredients of avalanche formation, namely the amount of new snow and the snowpack stratigraphy. The spatial variability of snowfall is mainly controlled by altitude but shows also a dependence on longitude and latitude. To understand this multivariable dependence, a method partitioning the simulated variability into elevation-related and position related variabilities is proposed. The PCA shows that up to 82% of the variance of the point sets (longitude, latitude, altitude, amount of new snow) is explained by one factor for certain snowfall events, which highlights the directionality of meteorological fluxes. The synthesise of stratigraphic information requires a method to compute metric between snow profiles. To this purpose, a recently developed matching algorithm was used. With this metric and agglomerative clustering, a few snow profiles characterizing the whole simulated data could have been successfully identified. These profiles well capture horizontal snow patterns identified after snowfall event and the wind effect on the snow properties. This study constitutes the first attempt to synthesise stratigraphic features as such a high spatial variability. It is however limited by the capability of AROME/Crocus whose resolution is still rough to capture wind-affected snow transport.

Keywords: simulations, Principal Component Analysis, matching, Dynamical Time Warping, clustering, snow profiles, spatial variability

Abstract

[Français] Les systèmes numériques de prévision météorologique en montagne à une résolution kilométrique offrent de nouvelles perspectives quant à l'évolution du manteau neigeux pour la prévision de risque d'avalanche. Dans cette étude les simulations quotidiennes du modèle météorologique Applications of Research to Operations at Mesoscale (AROME) à 1.3-km de resolution sur les Alpes françaises sont utilisées pour fournir des renseignements sur les conditions atmosphériques au modèle de manteau neigeux Crocus. L'orientation et la pente ne sont pas considérées dans les simulations tout comme le transport de neige par le vent. Ces simulations produisent de large quantité de données qui doivent être synthetisées sans perdre la qualité de l'information sur la variabilité spatiale du manteau neigeux, paramêtre critique à la prévision de risque d'avalanche. Cette étude utilise des outils statistiques comme l'Analayse en Composante Principale (ACP) et les techniques de clustering pour caractériser la variabilité spatiale du manteau neigeux à l'échelle du massif. Ces outils ont été utilisés sur les deux variables principales influençant la formation d'une avalanche: la neige fraiche et la stratigraphie du manteau. La variabilité du manteau neigeux est principalement controllée par l'altitude mais dépend également de la longitude et la latitude. Pour mieux compendre cette dépendance multi-variable, une méthode est développée pour différencier la variabilité causé par l'altitude ou celle liée à la position dans le massif. L'ACP montre que jusqu'à 82% de la variance du nuage de points (longitude, latitude, altitude, quantité de neige fraiche) pour certains massifs et épisodes neigeux peut être expliquée par le seul premier composant de l'ACP qui rend compte de la direction principale des flux météorologiques. La synthèse des informations stratigraphiques exige une méthode permettant de calculer la distance entre chaque profiles. Dans ce but, une méthode recemment dévoleppée de matching est utilisées. Grâce à cette distance et la méthode de clustering, des profils représentatifs de la strtigraphies du manteau neigeux pour chaque cluster ont été identifiés. Ces profils capturent les structures horizontales du dépôt de neige fraiche identifiées après des épisodes neigeux ainsi que l'effet du vent sur les propriétés des cristaux de neige. Cette étude est une première approche dans la synthèse d'informations stratigraphiques du manteau neigeux pour une si grande variabilité spatiale. Ces outils sont pour l'instant limités compte tenu des incertitudes provenant des simulations AROME/Crocus.

Mots-Clés: simulations, Analyse en Composante Principale, Dynamical Time Warping, matching, clustering, profils de neige, variabilité spatiale

Acknowledgements

Je tiens à remercier tout particulièrement mes deux maîtres de stage, Vincent VIONNET et Pascal HAGENMULLER, pour leurs conseils avisés et experts concernant mon sujet de stage pendant ces 5 mois passés ensemble. Sans eux, la réalisation de cette étude n'aurait pas été possible. Merci également pour le temps passé à la relecture du rapport et des nombreuses corrections et remarques pertinantes apportées.
Je remercie Isabelle GOUTTEVIN d'avoir acceptée d'être examinatrice de ce travail.
Je remercie mes responsables de Master, Didier VOISIN et Christophe BRUN pour leur suivi tout au long du stage.
Je remercie également Daniel GOETZ pour la description détaillée des épisodes précipitants sur notre période d'éude qui nous a été très utile.
Merci à Cécile COLEOU pour les discussions sur la prévision du risque d'avalanche et son regard avisée sur les évènements intéressants de la saison pour tester nos méthodes.
Merci à François TUZET, Yves LEJEUNE, Yannick DELIOT et Vincent VIONNET pour les sorties sur le terrain au Lautaret, Col de Porte et Col du Lac Blanc afin de voir la neige (en vrai!).
Merci à mes co-bureaux, Louis QUENO et Léo VIALLON pour la bonne ambiance, studieuse mais faite aussi d'entre-aide et de rigolade qui a contribué à la bonne ambiance de travail pendant ce stage. Je remercie tout particulierement Louis pour ses nombreux coups de main dans les moments "short in time" de la fin de l'écriture de ce rapport.
Je remercie bien évidement toutes les personnes du CEN et de Météo-France ayant contribuées de près ou de loin à cette étude. J'ai beaucoup apprecié les moments passés à vos côtés autour de discussions scientifiques, à table ou simplement autour d'un café.
Enfin merci à mes amis et mes parents pour leur soutien, essentiel à la bonne réalisation de ce travail.

Contents

List of Figures

List of Tables

Chapter 1

Introduction and context

Avalanches and controlling factors

Avalanches are a major danger in mountainous areas that threatens human life and infrastructures. In many countries with seasonally snow-covered mountains, avalanche-forecasting services warn the public by issuing level of risk for a certain region (Schweizer et al., 2003). Avalanche triggering depends on complex interactions between terrain, snowpack, and meteorological conditions.
Terrain is an essential factor that is constant over time. A slope angle of higher than 30^o is usually required for dry snow slab avalanches (Schweizer et al., 2003). Temperature is an other decisive factor contributing to avalanche formation. Its effect on snow stability is complex since changes in air temperature affect snow stability in various ways (Schweizer et al., 2003). For large avalanches, new snow (precipitation) is the strongest forecasting parameter (Föhn et al., 2002) and is closely related to avalanche danger. Accumulation of a new snow of about 1 m during a storm is considered critical for the initiation of extreme avalanches; about 30–50 cm is critical for naturally released avalanches in general (Schweizer et al., 2003). Wind is often considered as the most active contributing factor after new snow. Loading by wind-transported snow can be fast and produces irregular deposits. Variations in wind speed and snow drift form layers of different density or hardness, creating stress concentrations within the layered snowpack variable. It is very variable over mountainous area (Gauer, 1999). Snow cover stratigraphy is recognized as the key contributing factor for dry snow slab avalanche formation. Indeed any loading by new or wind-driven snow or any temperature increase has no effect on snow stability if no weakness exists in either the old snow or at the old snow surface underlying the new snow. The properties of the overlying slab also have to be considered (McClung and Schweizer, 1999; Schweizer, 1993; Schweizer et al., 1998).

Spatial variability of the snow cover

A major challenge in seasonal snow cover studies in mountainous terrain is to take into account the high spatial variability of the snowpack, since it affects many phenomena in mountains and is an essential factor of avalanche formation (Schweizer et al., 2003). The spatial variability of the snowpack is observed at different scales and is mainly caused by the spatial variability of atmospheric conditions, on the same range of scales. The regional climate determines the main synoptic weather patterns which contribute to the snow cover build-up. The evolution of the local meteorology is also driven by the mountainous complex architecture (Chow et al., 2012). Within a mountain range at a given elevation, snowfall is following the principal meteorological fluxes which control the spatial variability of the snow cover distribution. At a smaller scale (less than 100 m), processes like wind-induced erosion (Pomeroy and Gray, 1995), avalanches (Schweizer et al., 2003) or preferential deposition of snowfall on the leeward slopes (Lehning et al., 2008) play a decisive role of the snow distribution (e.g., Mott et al., 2010).

Snowpack modelling in alpine terrain

The description of the snowpack variability through snowpack modelling is highly dependent on the spatial resolution of the atmospheric forcing. For operational avalanche hazard forecasting in the French Alps, this variability is currently represented by classes of elevation, slope and aspect of about 1000 km^2. The detailed snowpack model SURFEX/ISBA/Crocus (Vionnet et al., 2012), mentioned as Crocus hereafter, is operational within the SAFRAN–SURFEX/ISBA/Crocus–MEPRA model chain (Durand et al., 1993; Lafaysse et al., 2013) for avalanche hazard forecasting. The meteorological analysis and forecasting system SAFRAN Système d'Analyse Fournissant des Renseignements Atmosphériques à la Neige (Analysis System Providing Atmospheric Information to Snow; Durand et al., 1993) provides relevant meteorological variables affecting the snowpack evolution, with a dependence on the elevation within these mountain ranges. It uses a conceptual representation of the topography and work at the so-called massifs scale. Each massif is considered to be climatological homogeneous (Durand et al., 1993). This representation is a limitation for snowpack simulations in mountainous terrain due to the complex topography which influences the development of an heterogeneous local meteorology.
For snowpack simulations in moutainous terrain, kilometric atmospheric informations offer potential to capture an important part of the intra-massif snowpack variability. Distributed simulations (i.e. on a regular spatial grid) of atmospheric forcing has been recently the object of many studies, building on the development of Numerical Weather Prediction (NWP) models of increasing resolution. Bellaire et al. (2011, 2013) performed snowpack simulations in Canada with the detailed snow cover model SNOWPACK (Bartelt and Lehning, 2002), driven by the 15-km resolution regional NWP model GEM15 (Mailhot et al., 2006), with a view to forecasting avalanche hazard. Bellaire et al. (2014) in New Zealand for avalanche hazard forecasting, uses NWP model ARPS (Advanced Regional Prediction System; Xue et al., 2000) at 3 and 1 km horizontal resolution to drive SNOWPACK. Horton et al. (2015) demonstrated the benefits of running SNOWPACK with the 2.5-km resolution NWP model GEM-LAM (Erfani et al., 2005) for specific studies of snowpack stability (surface hoar formation). The snowpack variability can also be simulated at scales of tens of metres, using adequate snowpack–atmosphere coupled models. Vionnet et al. (2014) used the coupled system Meso-NH/Crocus to study wind-induced erosion of the snowpack, at a 50 m horizontal resolution, and Mott et al. (2014) used the atmospheric model ARPS at a 75-m horizontal resolution to study the orographic effects on snow deposition patterns.
Since 2008, Météo France developed the high-resolution system AROME (Application of Research to Operations at MEsoscale; Seity et al., 2011) which is operational at kilometer scale over France. It is a 1.3-km resolution NWP model. The kilometric resolution over the French mountains offers an alternative to the forcing of Crocus by SAFRAN, at higher resolution, but without a dedicated analysis system. AROME has been evaluated to drive Crocus in mountainous terrain (Vionnet et al., 2016; Quéno et al., 2016). AROME/Crocus presents an overestimation of the Snow Water Equivalent (SWE) and snowfall at high altitude but a better representation of snow spatial distribution. The model underestimates the accumulation which is counter-balanced by an underestimation of the intensity of ablation processes. AROME forecasts at kilometer scale has the potential to produce reliable and continuous snowpack simulations over the French Alps (Vionnet et al., 2016; Quéno et al., 2016). AROME/Crocus simulations have never been evaluated in the context of avalanche hazard forecasting. The snow profiles describing the snowpack layering have been simulated but have never been analysed.

Use of model in support of avalanche hazard forecasting

Météo-France is in charge of the avalanche hazard forecasting since 1970. Forecasters produce evaluation of the avalanche risks for the French Alps at massif scale. The geometry of this entity is the same as the SAFRAN analysis. It consists in evaluating the stability of the snow pack and

its evolution along the winter. For this purpose, forecasters combine several informations such as: the meteorological forecast for the concerned areas; snowpack observations coming from professionals working in ski resort or automatic stations (so-called "Nivose") and results of numerical modelling dedicated to the avalanche risk forecast.
So far, the forecasters used the results of SAFRAN/Crocus as a decision-making aid to produce the avalanche bulletin. AROME/Crocus provides amount of new snow and stratigraphy information at a finer scale but has never been used for avalanche hazard forecasting. Indeed AROME/Crocus simulations are far more complicated to interpret as a large quantity of data is generated over the French Alps. SAFRAN analysis works with 8 to 12 elevation bands of 300 m per massif whereas AROME uses approximately 600 grid points at 1.3-km resolution for a 1000 km^2 massif. This corresponds to approximately sixty times more informations. Synthesise tools need to be developed for the exploitation of theses simulations by the forecasters.

Synthetise tools to analyse spatial variability

Two kinds of tools are generally used to synthesise information. Physically based models such as Modèle Expert d'Aide à la Prévision du Risque d'Avalanche (MEPRA Giraud, 1992) add mechanical properties of the snowpack simulated by Crocus and analyse the snow profiles in term of natural or accidental stability. It can provide a synthesis a avalanche risk at the massif scale (e.g. Rousselot et al., 2010). MEPRA proposes a quantitative evaluation of the avalanche hazard at this scale. Hybrid expert systems have been developed coupling expert systems with statistical methods (e.g. Schweizer et al., 1994; Bolognesi et al., 1994). The models uses weather and snow cover data as input parameters and the system evaluates the level of avalanche danger in a given region.
Several studies use statistical approach to investigated factors influences spatial and temporal distribution the snow cover in response to atmospheric circulation (Esteban et al., 2005). Spanish studies quantify the changes in the patterns of weather types affecting snowfall (Esteban et al., 2005). Silverman et al. (2013) performed PCA to find principal processes driving the spatial distribution of the precipitation. Hevesi et al. (1992) has performed cokriging and variogram to better estimate precipitation in mountainous terrain. Grünewald et al. (2013) uses statistical model by applying multiple linear regressions to study the snow depth distribution on alpine terrain. In other domains (e.g. respectively representation of low-pressures centres,wind erosion events, precipitation patterns; Kidson, 1994; Ekström et al., 2002; Romero et al., 1999) Principal Component Analysis and clustering reveals to be useful tools to identify spatial distribution of variables.

Goal of the study

Using the results of AROME/Crocus simulations, we want to develop analysis tools to synthesise information on the spatial variability snow cover and to propose diagnostics useful for forecasters. To this purpose, multivariate statistical methods are computed to some key variables for avalanche hazard forecasting: the amount of new snow, position on the grid, elevation and variables describing the snowpack stratigraphy. Following the previous studies the covariance matrix, PCA and clustering are used. For stratigraphic profiles, the analysis is more complex since this data can not be reduced to single scalar. We employed more complex methods such as recently developed matching algorithm (Hagenmuller and Pilloix, 2016) and agglomerative clustering to identify crucial features.
This thesis is organised as follows. We first introduce the geographical characteristics of the study area and describes notable snowfall events of winter 2016-2017. In this section, the model AROME/Crocus is exposed. The statistical methods are then presented. The results of this study are exposed in the following and discussed. Finally, we conclude and highlight the outlooks.

Chapter 2

Data

2.1 Study area and time period

This study focuses on the French Alps, the natural border which separates France from Italy and Switzerland (Figure 2.1). The domain of study extends from 43.875 to 46.5°N latitude and from 5 to 8°E longitude. Snow patterns in the French Alps are characterized by a marked declining gradient from the north-western foothills to the south-eastern interior regions. This domain is partitioned into massifs defined as area with a climatological homogeneity.
The period of study goes from November 2016 to April 2017. In this season, six snowfall episodes with long dry period in between has been retained to test the methods developed. Tab. 2.1 The illustrative maps on Fig. 2.2 allows to a an approximate idea of the distribution of precipitation. The maps are built from sparse observations and then interpolated. Due to this construction and the mountainous terrain, there are a lot of uncertainties.

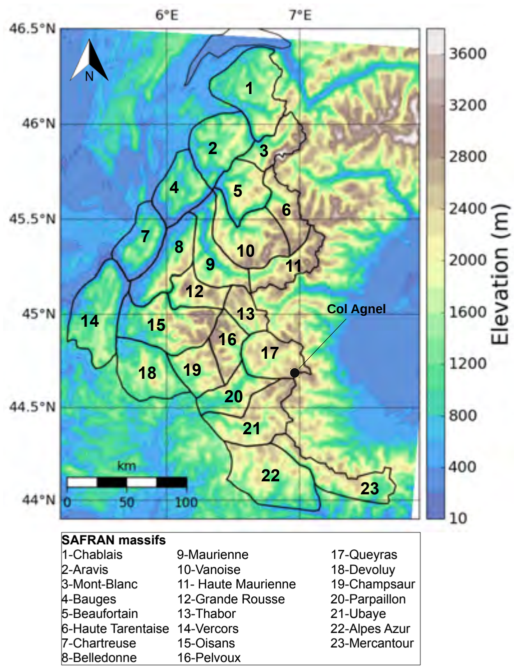

FIGURE 2.1: Map of simulation domain showing the topography at 1.3km-grid spacing using AROME. Contour of SAFRAN massifs used for the avalanche hazard forecasting are delimited by the black line. The black dotlocalised the Col Agnel station which is used in this study

2.2 Snowpack simulations

In this study, the Numerical Weather Prediction (NWP) system AROME at 1.3-km grid spacing is used to drive the snowpack model Crocus and to simulate the snowpack evolution over the French Alps during winter 2016/2017. SAFRAN reanalysis system is used to initialise Crocus before the period of interest. Crocus uses as input air temperature at a given height above the ground, specific humidity, wind speed at a given height, surface incoming short-wave (SW) and long-wave (LW) radiation, solid/liquid precipitation rate. The two types of atmospheric forcing used in this study -AROME forecast and SAFRAN analysis- are described in this section. The snowpack model Crocus is also presented.

2.2.1 AROME: kilometric resolution NWP system

AROME is the high resolution NWP system operational and mainly developed at Météo-France (Seity et al., 2011; Brousseau et al., 2016). It explicitly models the physics and dynamics of the atmosphere and is able to assimilate meteorological data. It is used by forecasters since December 2008. With a 1.3-km horizontal grid mesh AROME (since April 2015) is designed for short-range

Year	Date	Description
2016	5-14 Nov.	Atlantic perturbation coming with snow and rain with cold temperature. The rain/snow limit is situated on average at 1100-1200 m a.s.l. This event concerns all French Alps;
	18-25 Nov.	Perturbation from South-West and then South with important Foehn wind on the Northern Alps. This event is then characterised by an important flux coming from the East with an extraordinary intensity along the Italian border;
	19-20 Dec	Mediterranean perturbation follow by Foehn event along Italian border;
2017	3-9 Feb	Perturbation coming from the Atlantic with wind at the beginning. Rain/snow limit ranges between 700 and 1600 m. The precipitation during this event evolves between 65 and 130 mm everywhere.
	28 Feb.-7 Mar.	Atlantic perturbation with a lot of wind (evolving in gusts; up to 142 km/h in altitude). The rain/snow limit is situated between 500 and 1900 m (precipitation in Northern Alps: 170-190 mm to 90-110 from North-West to South-East; precipitations Southern Alps: 80-100 mm to 50-60 mm from West to East.
	22-25 Mar.	Perturbation from South to South-East with a rain/snow limit around 1700-1900 m evolving to 1200 m at the end of the event. The precipitations during this event in the Northern Alps represents 15-20 mm to 30 mm from the North-West to the South-East.

TABLE 2.1: Description of the important snowfall events occurring during the winter 2016-2017

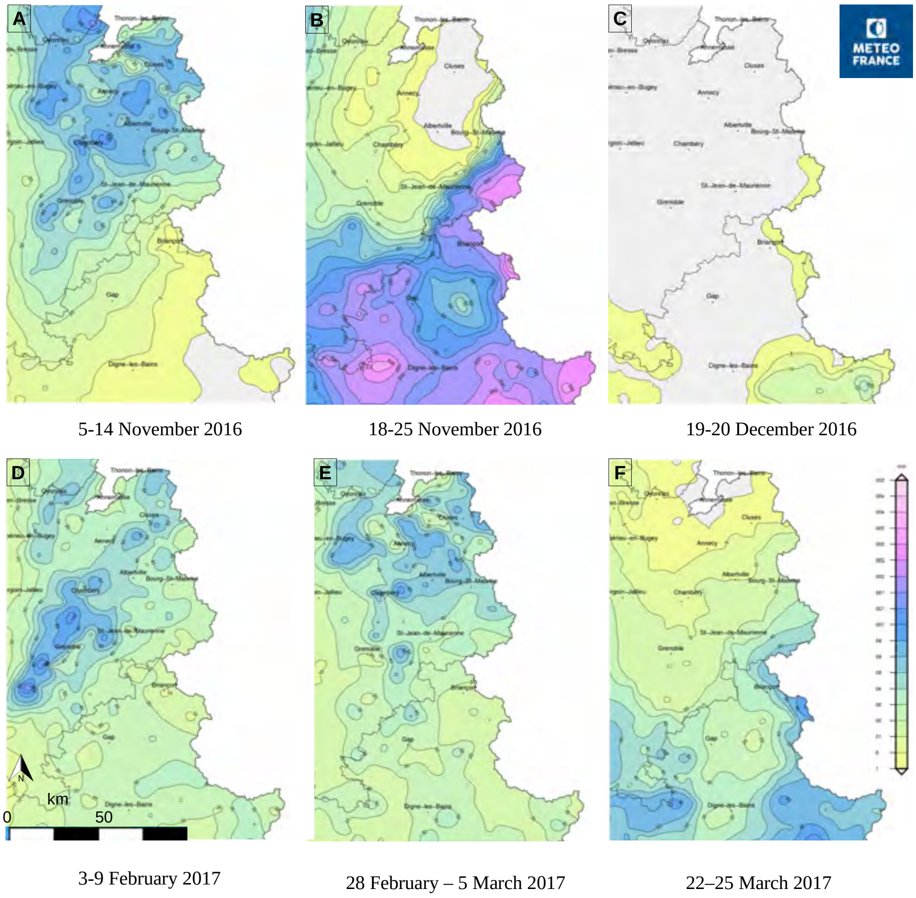

FIGURE 2.2: Total precipitation observed for snowfall events of winter 2016/2017. The maps come from Meteo-France data base: http://climascope.meteo.fr

forecast and aims in particular at improving the forecasts of small-scale processes in alpine terrain such as orographic precipitation or Foehn wind. Recent studies (Vionnet et al., 2016; Quéno et al., 2016) have evaluated the quality of AROME forecasts at kilometre scale in the Alps and the Pyrénées and have discussed the ability of AROME to drive snowpack simulations in these regions.

AROME provides forecasts with a 42-h lead time for 00 and 12 UTC analysis time and with a 36-h lead time for 06 and 18 UTC analysis time. The output grid in this study is restricted over the French Alps from 43.875^o-46.5^{o}N,5^o-8^{o}E (originally 41^o-51.51^{o}N and 6^{o}W-10.5^{o}E). In term of atmospheric forcing, temperature, specific humidity are taken at 2 m diagnostic level. The wind speed is taken at 10 m diagnostic level. Radiative budget is obtained thanks to cumulated values of different fluxes. Precipitation are obtained in the same way. The hourly atmospheric forcing for snowpack simulations are obtained from daily forecasts issued at the 00 UTC analysis time. As in Vionnet et al. (2016) successive 6-9-h lead time forecasts are combined together to generate a continuous atmospheric forcing from 1 November 2016 to 1 April 2017.

2.2.2 SAFRAN: reanalysis system

SAFRAN analysis system (Durand et al., 1993) is operational at Météo-France for avalanche hazard forecasting (Lafaysse et al., 2013) within the chain SAFRAN/SURFEX/Crocus. It has been developed to provide relevant atmospheric forcing to the snowpack model Crocus. Combined with Crocus and MEPRA, it is used as an help for the forecasters to produce an avalanche bulletin. SAFRAN reanalysis (Durand et al., 2009a,b) is a combination of weather data available from observation sources and NWP simulations at 40-km grid spacing. It includes hourly atmospheric forcing data. The analysis is made on 23 areas of the French Alps known as massif. Each area is supposed to present climatological homogeneity (Durand et al., 1993). The reanalysis is available in 300-m elevation step. The spatial definition has limitations in mountainous area due to the variable meteorology associated with the complex topography (Vionnet et al., 2016; Quéno et al., 2016). In our study SAFRAN forcing variables are interpolated over the 1.3-km grid of AROME to provide initial conditions to Crocus from 1 August 2015 to 1 November 2016 (see 2.2.3 for more detail).

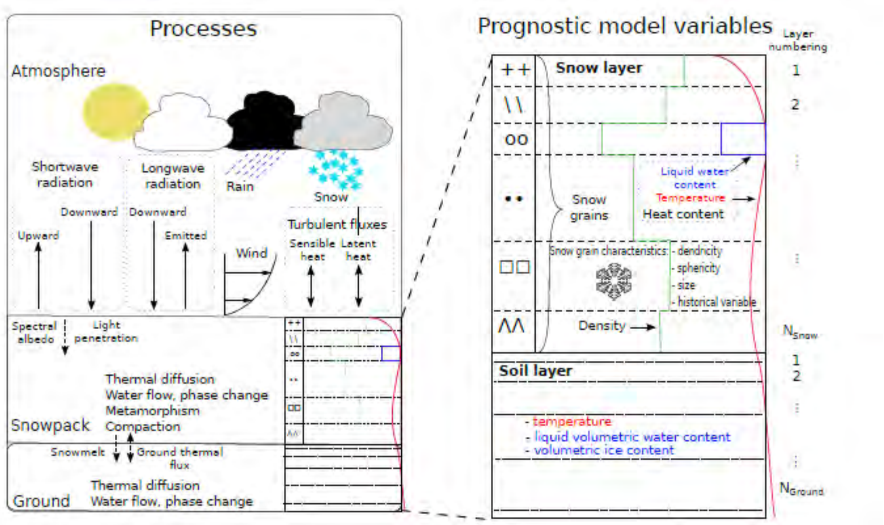

FIGURE 2.3: Main physical processes and model variables of SURFEX/Crocus (Vionnet et al., 2012)

2.2.3 Crocus: snowpack model

Crocus is a one-dimensional multilayer physical snow scheme which simulates metamorphism and layering of the snowpack (Brun et al., 1992; Vionnet et al., 2012). It is coupled with Interactions between Soil, Biosphere, and Atmosphere (ISBA) (Giard and Bazile, 2000) land surface model within SURFEX simulation platform (Masson et al., 2013). The required are air temperature, specific humidity, wind speed; incoming radiation: direct and diffuse short-wave (SW) and long-wave (LW); precipitation rate split between rain and snow; atmospheric pressure. These informations can be derived from local observations, atmospheric models or reanalysis. Crocus simulates the evolution of the snowpack as a function of energy and mass-transfer between the snowpack and the atmosphere. The exchange between the snowpack and the underlying ground is also taken into account in the simulations. (Vionnet et al., 2012) (Fig. 2.3).
Soil proprieties has a prescribed composition of $\frac{1}{3}$ clay and $\frac{2}{3}$ sand as in the operational chain for avalanche hazard forecasting (Lafaysse et al., 2013). Distributed snowpack simulations are performed over the AROME forcing grid at 1.3-km resolution. Interactions with the vegetation are considered only in forested areas. The snow fraction is set to 1 whenever snow is present on the ground. The 1.3-km grid is too coarse to represent the distribution of slope and aspect found in alpine terrain. The slope on the simulation points is set to zero. The wind-induced snow transport is not simulated but wind can affect snow atmospheric precipitation. Snowpack simulations are performed from 1 November 2016 to 1 April 2017.
For the study, the amount of new snow $HNW(period)$, Specific Surface Area (SSA) and density

are the prior interest. The amount of new snow is quantified by the variable $HNW(period)$ defined as the snow water equivalent of snow layers which were formed during a certain period. This variable integrates new snow but also melting and sublimation processes. The SSA is a quantitative metric defined as the total area at the ice/air interface in a given snow sample per unit mass. SSA is key variable indicating snow metamorphism. The SSA of fresh snow is high and it decreases with time because the grains round up. The fresh snow has a very low density and it increases with time because of the metamorphism. However the increase, of the density is not uniform and also depends on melting processes and temperature gradient metamorphism.

Chapter 3

Method

3.1 Spatial variability of the amount of new snow

Schweizer et al. (2003) describes five essential factors that contribute most to avalanche danger. In this study, we focuses essentially on new snow after snowfall episode and snowpack stratigraphy. The methods presented in this section aim to develop analysis tools for AROME/Crocus output simulations to synthesise the spatial variability informations. In the first part of the section, we present the method which allows us to partition the spatial variability into, on one hand, the dependence to the longitude and the latitude; and on the other hand, dependence to the altitude.

3.1.1 Horizontal and vertical dependence of HNW

In mountainous terrain, the snowfall distribution over a given area is strongly influenced by elevation (Grünewald et al., 2014). Enhanced precipitation are also expected on the upwind side of mountain ranges and less precipitation relative to local elevation are found on the downwind side. Principal meteorological fluxes controls the snow cover variability resulting of precipitation patterns. We propose a method to detrend the amount of new snow from elevation effect for a given geographical entity,GE (e.g. massifs). To this purpose, the mean of the $HNW(period)$ -$\overline{HNW(period)}^{GE}$- over the geographical entity per altitude band of 100 m -AROME vertical resolution- is calculated. We interpolate the value between each altitude band to have $\overline{HNW(period)}^{GE}$ for every altitude (Fig. 3.1). This value is then subtracted to the value of the $HNW(period)$ on each simulation points according to its altitude (Eq. 3.1). The $HNW_{det}(\tilde{period})(i,j)$ is given in percentage for a better understanding of the results.

$$HNW_{det}(\tilde{period})(i,j) = \frac{HNW(period)(i,j) - \overline{HNW(period)}^{GE}(z_{i,j})}{\overline{HNW(period)}^{GE}(z_{i,j}} \times 100 \qquad (3.1)$$

where i and j are the coordinates of the simulation points and z is the altitude.

3.1.2 Covariance matrix and Principal component analysis (PCA)

The PCA is computed to analyse the complex relationship existing between the snowfall quantity, the altitude and the position in the massif.

Introduction

The PCA is used to reduce the dimension in a dataset by finding patterns within it. It is first developed by Pearson (1901) but the version presently used is developed by Hotelling (1933). The PCA finds linear combinations of the initial variables which explain the most of the variance of the data. These combinations are called Principal Component (PC) (Fig. 3.2).

The PCA proposes a geometric representation of the data coming from a table with 4 variables

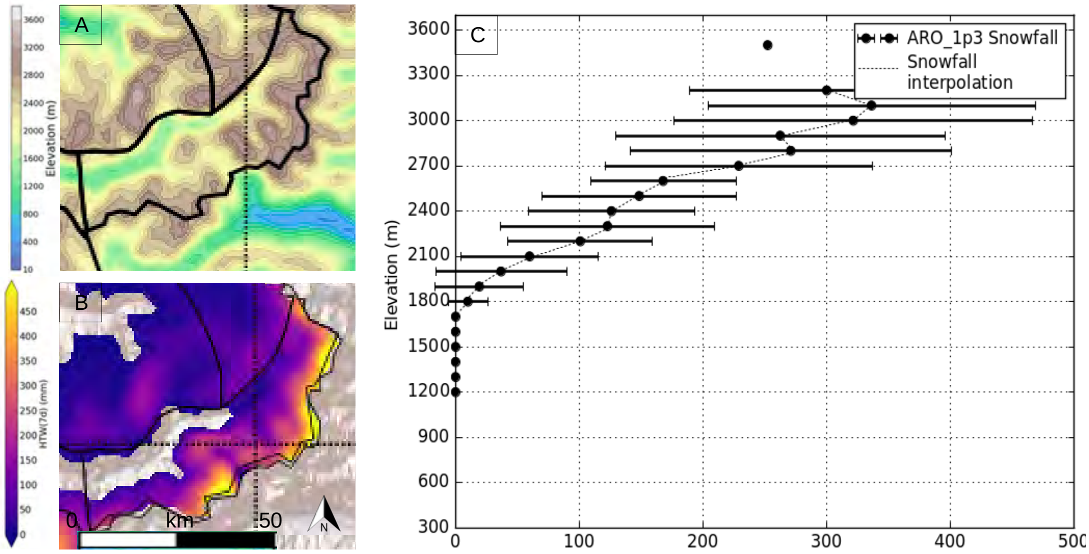

FIGURE 3.1: $\underline{HNW(period)}$ of the Haute-Tarentaise massif as a function of altitude. The black dots represent $\overline{HNW(period)}$ calculated for 100-m elevation band. The dashed line represents the interpolation computed between each 100-m elevation. The value of $HNW(period)$ comes from AROME/Crocus simulations.

and n individuals -number of simulation points within a massif (Eq. 3.2). In this study, we perform the PCA on the variables SWE, longitude X, latitude Y and altitude Z. The PCA is performed for each massif.

$$\mathbf{S} = \begin{array}{c} \begin{array}{cccc} X & Y & Z & HNW(period) \end{array} \\ \begin{bmatrix} X_{11} & Y_{12} & Z_{13} & HNW(period)_{14} \\ X_{21} & Y_{22} & Z_{23} & HNW(period)_{24} \\ \vdots & \vdots & \vdots & \vdots \\ X_{n1} & Y_{n2} & Z_{n3} & HNW(period)_{n4} \end{bmatrix} \end{array} \begin{array}{c} pix_1 \\ pix_2 \\ pix_3 \\ pix_n \end{array} \tag{3.2}$$

With pix corresponds to the pixels of each massif and n the number of it.

Procedure

In this study, the PCA is performed as following:

- The data set is normalised. The mean of each variables is subtract to the variables and they are divided by the standard deviation of each variable.
- The covariance matrix, $\sum$ is built. It has the 4×4 dimension since there are 4 variables studied. The covariance between variables X and Y is defined as:

$$Cov(X,Y) = \frac{\sum_{i=1}^{n}(X_i - \overline{X})(Y_i - \overline{Y})}{n-1} \tag{3.3}$$

The eigenvalue is a scalar which has a corresponding eigenvector. The corresponding eigenvalue is a number that indicates how much variance there is in the data along the corresponding eigenvector. Mathematically the principal components are the eigenvectors of the covariance matrix of the original dataset. The eigenvector with the largest eigenvalue is called the first principal component. As this matrix is symmetric, the eigenvectors are

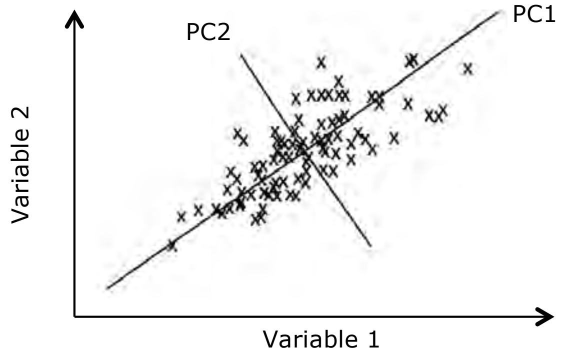

FIGURE 3.2: Exemple of the PCA computed in 2D. The first compenent explains the most of the variance.

orthogonal. It corresponds to the direction with the greatest variance in the data. The components are ordered from the highest eigenvalue to the lowest eigenvalue.

- Then we keep only the $P < 4$ components to keep to form a matrix with these vectors in the columns. This matrix is called the feature vector. In this study, only one component was retained. This analysis was performed with the python package sklearn.decomposition.PCA.

3.2 Spatial variability of the snowpack stratigraphy

This section is dedicated to the study of the snowpack stratigraphy and we present methods developed to define group of similar snow profiles together and to identify representative profiles of the defined group.

3.2.1 Clustering

Cluster analysis enables to group the data set into different categories. Similar objects are assigned to the same group.

Agglomerative clustering

The agglomerative clustering method constructs the cluster by recursively partitioning the instance in bottom-up fashion. Each object initially represents a cluster on its own. Then clusters are successively merged based on a certain inter-cluster distance until the desired cluster structure is obtained (Fig. 3.3). There are many ways to compute clusters e.g. K-means, mean-shift, DBSCAN. We choose agglomerative clustering because it can be applied to any dataset with a pairwise distance metric. It does not require the points of dataset to be in a euclidean space, on the contrary to afore mentioned method.

Metric used for clustering

This method requires two main ingredients:

- a distance between two elements of the data set. This is called the element distance.

- a method to compute the distance between two clusters composed of several elements and based on the local distance. This is called the linkage method. This distance is used to determine which clusters should be joined.

In this study the clustering is based on the distance matrix computed with the Distance Time Warping algorithm describes in the section 3.2.2. Presently we used the Ward method as a link-

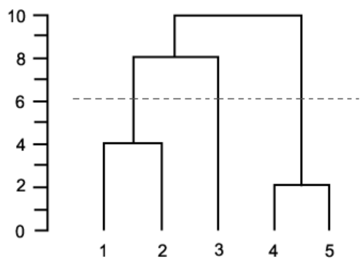

FIGURE 3.3: Agglomerative clustering method. For this method, each pixels represents one cluster (bottom of the figure) and they are then merged together until the number of cluster is obtained, 3 in this case (branches which cross the dashed horizontal line)

age method. The Ward distance between two clusters is the sum of square of the local distance between all possible pairs of elements. It is a variance-minimizing approach. The merge between two clusters with the lowest ward distance is chosen. This rule tends to produce clusters with approximately equal size. There is no connectivity constrains applied to the clustering method: clusters that are not adjacent can be merged together.
This analysis was performed with the python package sklearn.cluster.AgglomerativeClustering.

3.2.2 Matching

The matching method allows to align snow profiles with each other and so the pairwise distance between snow profiles essential for the clustering. The idea is to consider that the depth of the snowpack is an adjustable parameter which can be transformed to match comparable profiles. In this way, the profiles that share the same crust or weak layers but at different depths can be recognized as similar. The matching is used to compute a distance between two profiles without according weight to the difference in terms of layer thickness but only accounting for the difference in terms of intensive properties such as SSA and density. In this work, the method is also used to combine many profiles of one set into a "mean" representative profile. This method has been developped for snow profiles by Hagenmuller and Pilloix (2016). The algorithm uses the DTW (Dynamic Time Warping) (Sakoe and Chiba, 1978) which is described in this section.

Dynamic Time Warping (DTW) algorithm

Dynamic Time Warping is a well-known technique to find an optimal alignment between two given sequences under certain conditions (Sakoe and Chiba, 1978). Intuitively the sequences are warped in a non-linear fashion to match each other (Fig. 3.4).
The DTW method compare two sequences of discrete signal $S = (s_1, s_2, ..., s_N)$ and $T = (t_1, t_2, ..., t_M)$.
The DTW method requires a local distance measure. In this study, we used the square of the difference:

$$d_{i,j} = (s_i - s_j)^2 \tag{3.4}$$

Typically $d(i, j)$ is small if i and j are similar to each other. Otherwise the distance is large. To evaluate the local cost measure for each pairs of elements of the sequences S and T we compute

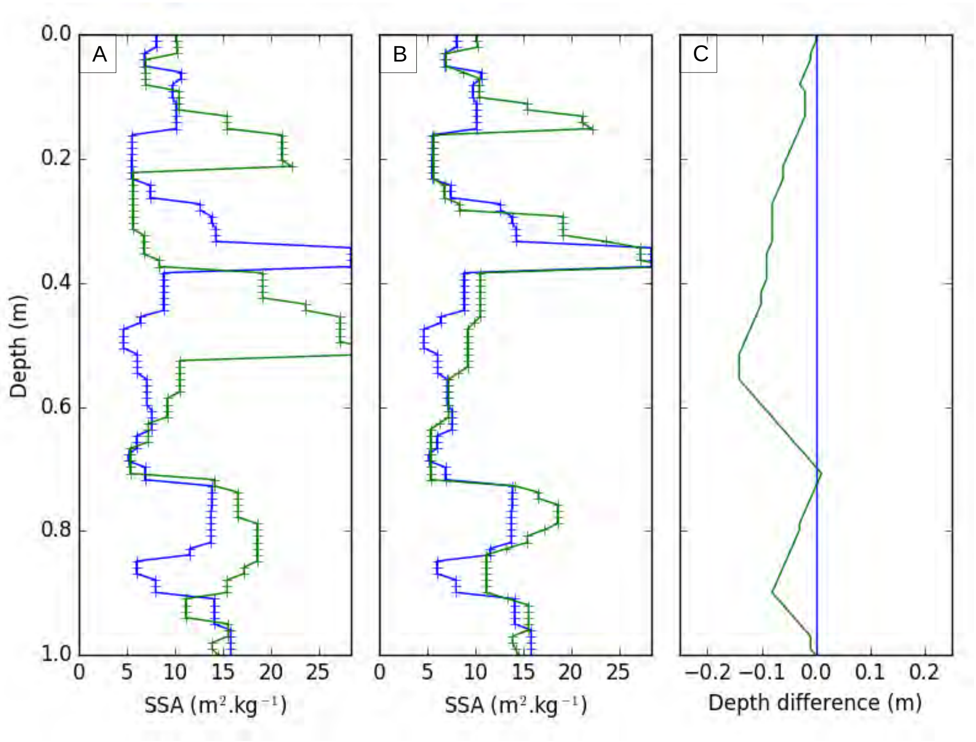

FIGURE 3.4: Initial profiles of SSA A) re-interpolated on a regular grid, B) transformed profiles so their distance is minimized. The figure C) represents the depth transformation of the profiles between this two steps. The blue curve is associated the reference profile and the green one to the matched profile.

the accumulated cost matrix D. The goal of this method is to find the optimal alignment between S and T having a minimal overall cost.
The (N, M) warping path is the sequence $p = p_1, ..., p_L$ with $p_\ell = n_\ell, m_\ell \in [1 : N] \times [1 : M]$ for $\ell \in [1 : L]$ satisfying the following condition:

- Boundary condition: $p_1 = (1, 1)$ and $p_\ell = (N, M)$
- Monoticity : $n_1 \leq n_2 \leq ... \leq n_L$ and $m_1 \leq m_2 \leq ... \leq m_L$
- Step size condition: $p_{\ell+1} - p_\ell \in \{(2, 1), (1, 2), (1, 1)\}$ for $\ell \in [1 : L]$. The local paths have local slope with bounds $\frac{1}{2}$ or 2. It means that local layer thickness can be stretched up to 100% and shrinked up to 50%.

The accumulated cost matrix D is computed by recursion:

$$D(n, m) = min\{D(n-1, m-1), D(n-2, m-1)+d(x_n-1, y_m), D(n-1, m-2)+d(x_n, y_m-1)\}+d(x_n, y_m) \tag{3.5}$$

for $n \in [2 : N]$ and $M \in [2 : N]$.
The initial values are then (Fig. 3.5):

$$D(1, 1) := d(x_1, y_1) + d(x_0, y_0) \tag{3.6}$$

$$D(n, 0) := \infty \text{ for } n \in [1 : N] \tag{3.7}$$

$$D(n, 1) := \infty \text{ for } n \in [2 : N] \tag{3.8}$$

$$D(0, m) := \infty \text{ for } n \in [1 : M] \tag{3.9}$$

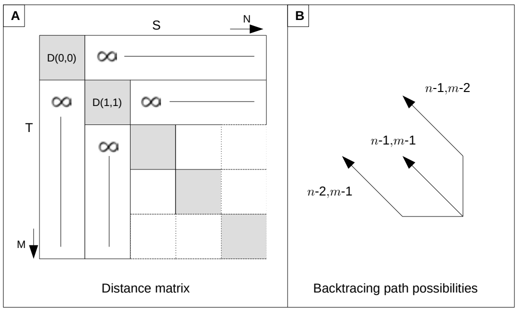

FIGURE 3.5: Matching method and backtracing possibility path. The figure describes A) the initialisation of the distance matrix and B) the different possible paths for the backtracing

$$D(1, m) := \infty \text{ for } n \in [2 : M] \tag{3.10}$$

As mentioned before , the snow layer thickness can not be locally stretched by more than 100% or shrinked by more than 50%. We also allow partial matching, which means that the bottom of the profiles are not necessarily matched. We impose that at least 60% of two profiles are matched together. Nevertheless, profiles with very different depth (more than 60%) are thus considered unmatchable and, in this case, we set an infinite distance between the profiles.

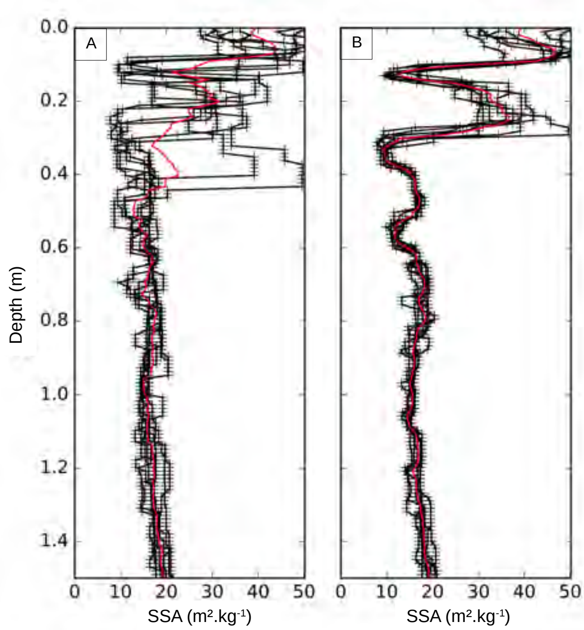

FIGURE 3.6: Auto-matching method. A) represents the the profiles of the one cluster where DTW has been already computed. B) represents the same profiles after 20 iterations for DBA method. The red line represents the averaged profile.

Auto-matching: DTW Barycenter Averaging (DBA)

The DTW algorithm has been adapted to match several profiles together. In this study, it is used to "auto-matched" profiles belonging to the same cluster. The DBA (Petitjean et al., 2011) is an approximate method solve this problem. It consists in iteratively refining an initially average sequence to minimize its sum of squared distance (DTW) to averaged sequences (Fig. 3.6). This sum is formed by single distances between each coordinate of the averaging sequence and coordinates of the sequences associated to it. The contribution of one coordinates of the average sequence to the total sum of squared distance is actually a sum of euclidean distances between this coordinate and coordinates of sequences associated to it during the computation of DTW. Minimizing the partial sum for each coordinate of the average sequence is achieved by taking the barycentre of this set of coordinates. The updated average sequence is defined once all barycentres are computed. This computation works in two steps:

- Computing the DTW between each individuals sequence and the temporary average sequence to be refined;
- Updating each coordinate of the average sequence as the barycentre of coordinates associated to it during the first step.

The proposed averaging method for DTW is a global approach that can average a set of sequences all together. The update of the average sequence between two iterations is independent of the order with which the individual sequences are used to compute their contribution to the update in question.

Chapter 4

Results

4.1 Spatial variability of the amount of new snow

SAFRAN/Crocus assumes homogeneous climatological conditions at the massif scale. Therefore the simulated intra-massif spatial variability is thus only a function of altitude for this model. However the distribution of the snow after a snowfall event is more complex due to the interaction with the topography and is still essential for avalanche hazard forecasting. AROME/Crocus showed its performance to simulate the spatial variability of the snow cover. In this study, the simulations are used to quantify the sensitivity of the amount of new snow -$HNW(period)$- to the altitude and the longitude/latitude. Two different approaches are considered.

4.1.1 Detrending of altitude effect

Figure 4.1A and 4.1C present distribution of the amount of new snow ($HNW(7d)$), simulated by AROME/Crocus for two snowfall events of winter 2016/2017. For the so-called East return event (Fig. 4.1A) strong snowfall occurred at the border with Italy, particularly on the Queyras, Mercantour and Haute-Tarentaise massifs. The $HNW(7d)$ is higher on the Eastern part of the massifs (e.g. 450 mm in the Eastern part of Haute Tarentaise; 500 mm in the Eastern part of Mercantour). This event affects more the Eastern part of the Alps compared to the Western part e.g. Grandes-Rousses compared to Mercantour. The high summits of the central French Alps e.g. Champsaur, Pelvoux, Oisans summits receives also high quantity with more than 350 mm.
For the second event (Fig. 4.1C) from the 28 February to the 5 March 2016, the snowfall is extended all over the French Alps. The amount of new snow is high in the Northern part of the Alps with $HNW(7d)$ up to 240 mm in the Chablais and the Mont-Blanc massif. The interior massifs -Champsaur, Maurienne, Oisans, Grandes-Rousses- are also affected by the event and particularly their summits.
These maps highlight contrasted patterns but we can not evaluate whether a higher amount of new snow is due to a high elevation or due to a specific "horizontal" position in the massif.
These conclusions motivate the application of the method described in the section 3.1.1. The geographical entity taken in to consideration to apply the method (see Eq. 3.1) is the massif. The border with Italy is strongly affected by the snowfall of November (Fig. 4.1B). For the East return event the East of Queyras and Haute-Maurienne massif receive 60% more snow than their western part for a given altitude. Intra-massif variability is clearly characterised for these massifs. For the event occurring at the beginning of March, clear patterns of snow distribution are also identified (Fig. 4.1D). The western part of the Grandes-Rousses massif presents a positive value of $\tilde{HNW}(7d)_{det}$ whereas its Eastern part presents a deficit of new snow. On Belledonne (Fig. 4.1D) the amount of new snow presents a positive anomaly on its Northern part which is not possibly identified on the map 4.1C.
As these maps (Fig. 4.1B, 4.1D) are based on the massif geometry, discontinuities are found at the border between two massifs. For example Figure 4.1B presents a positive anomaly at the South of the Ubaye massif (+40%) whereas we highlight a deficit of snow at the North of Mercantour at the

same rate (-40%). Using the massif as the geographical entity to detrend the effects of elevation, these maps are not valuable at the inter-massif scale.

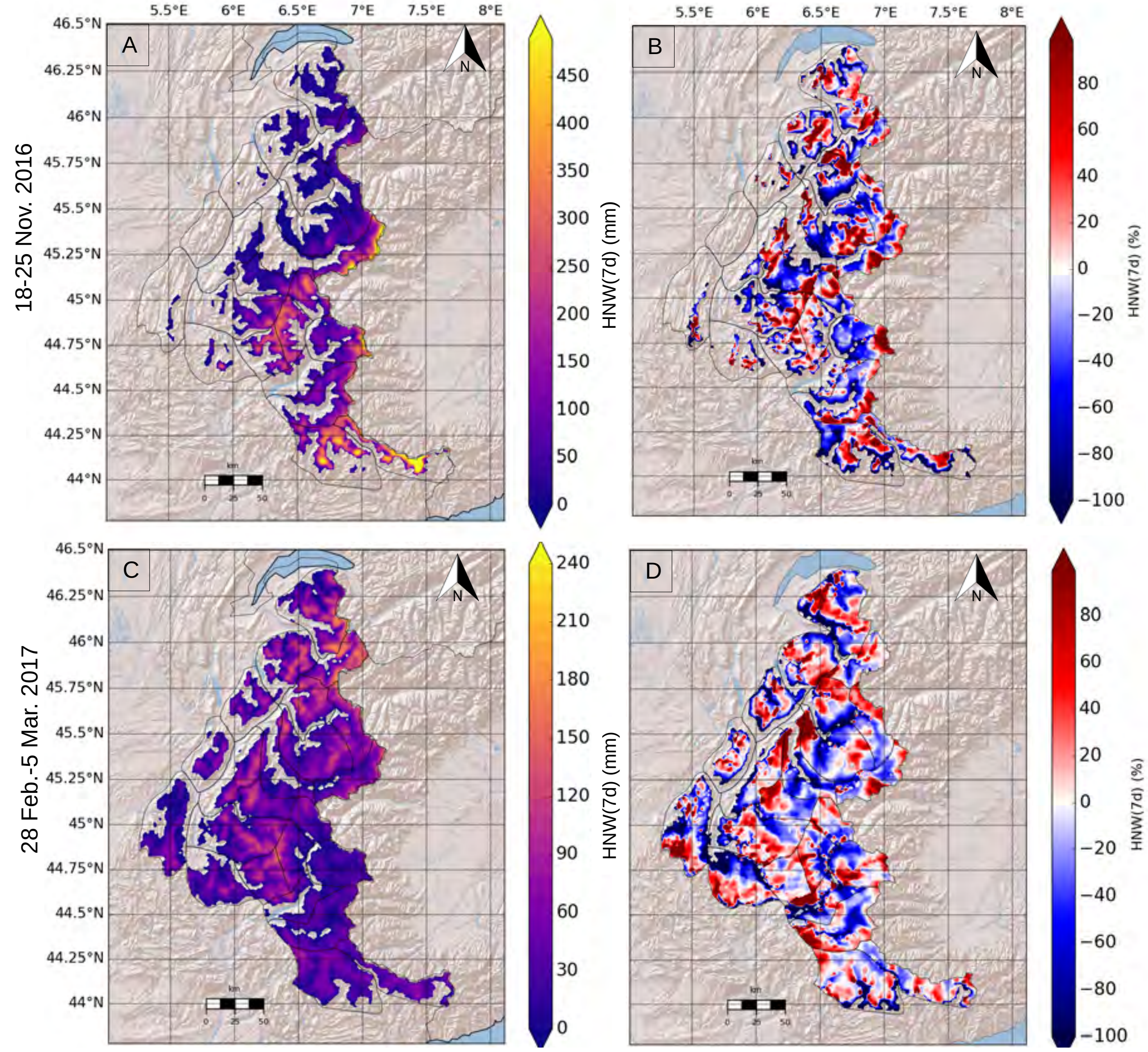

FIGURE 4.1: Maps of the amount of new snow for two events represented $HNW(7d)$ A,C) and $HNW(7d)$ distribution B,D). The method to detrend $HNW(7d)$ is applied at the massif scale.

4.1.2 Analysis of the covariance and principal component analysis

The covariance matrix and the PCA are computed to quantify the relative contribution of the altitude and the position in the massif to the $HNW(7d)$. The PCA is performed for each massif.

Covariance

The covariance matrix,$Cov(X, Y)$ is directly linked to the correlation matrix with the relation:

$$corr(X, Y) = \frac{Cov(X, Y)}{\sigma(X)\sigma(Y)} \quad (4.1)$$

where $corr$ is the correlation matrix and σ the standard deviation of each variable. As the variables are normalised in our study, these two matrix are equals.

Analysis of the covariance matrix allows to understand the relation between the longitude, latitude, altitude and the amount of snow after a snowfall event. Figure 4.2A shows the covariance matrix for the Queyras massif after the so-called East return event. The $HNW(7d)$ is strongly positively correlated to the altitude and to the longitude. It is slightly anti-correlated to the latitude. The altitude is correlated to the longitude with an important covariance factor. Regarding Fig. 4.1B the highest amount of snow are found in the Eastern part of the massif and the high summits of the Queyras massif (Fig. 2.1) are situated in the same part.
The covariance matrix is computed on the Grandes-Rousses massif after the snowfall event of March (28 February 2017 to 5 March 2017, Fig. 4.2B). Again, $HNW(7d)$ is strongly positively to the altitude and, with a less important correlation factor, to the latitude. It is slightly anti-correlated to the longitude. The altitude is however importantly correlated to the longitude. The covariance matrix describes the spatial patterns of the amount of snow retrieve on Fig. 4.1.
The covariance matrix correlates the variables to that describe the vertical architecture of the massif (position of the high summits) and the spatial patterns of the amount of snow.

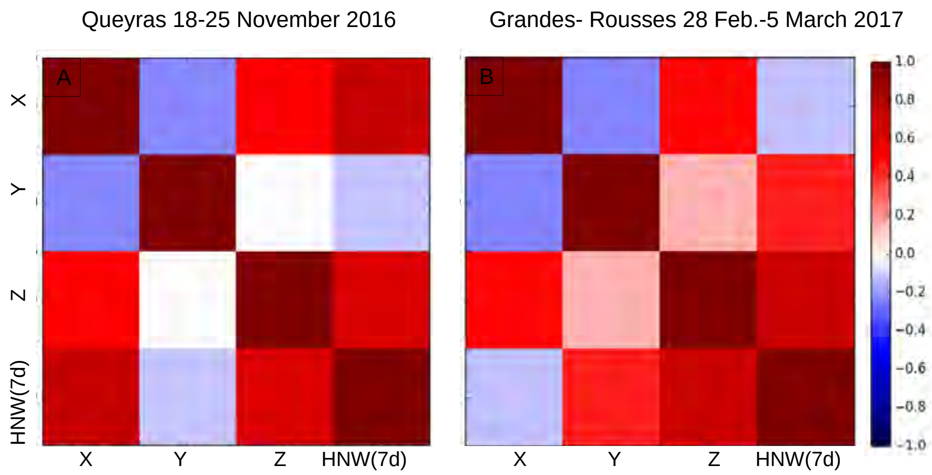

FIGURE 4.2: Covariance matrix in the A) the Queyras and B) Grandes-Rousses massif for respectively the event from 18-25 November 2016 and from 28 February to 5 March 2017. The covariance matrix gives the correlation factor between variables computed in the PCA: X (longitude), Y (latitude),Z (altitude) and $HNW(7d)$

Principal component analysis

The PCA used the covariance matrix to be perfomed. Figure 4.3 shows the results of the PCA for the first component PC1 for the same events as in section 4.1.1 for an easier comparison. The eigenvalue of $HNW(7d)$ is forced to be positive for a better understanding of the results (Fig. 4.3). The more red the square is, the more correlated the variable is with the component. On the contrary the more blue the square is, the more anti-correlated the variables are with the component. When the square is white, it means that the variable is not correlated with the component. We applied a restrictive condition for each massif. If the average value for the massif is lower than $\frac{3}{4}$ of the mean of the $HNW(7d)$ in the French Alps, the PCA is not computed for these massifs. It corresponds to the grey square on Fig. 4.3. We observe that the first component explains between 48% and 82% of the variance (Fig. 4.3B and 4.3D). This important value highlights the simplicity to explain the distribution of the amount of new snow. Indeed one linear combination is sufficient to explain a large part of the variability of the set of points (longitude, latitude, altitude and $NNW(7d)$). Simply, the four variables are situated along the same line on a 4D space. In this case the PCA allows a compact visualisation of the covariance matrix by representing only the three quarter of the variance for the majority of the massifs. For the both events, $HNW(7d)$ and the

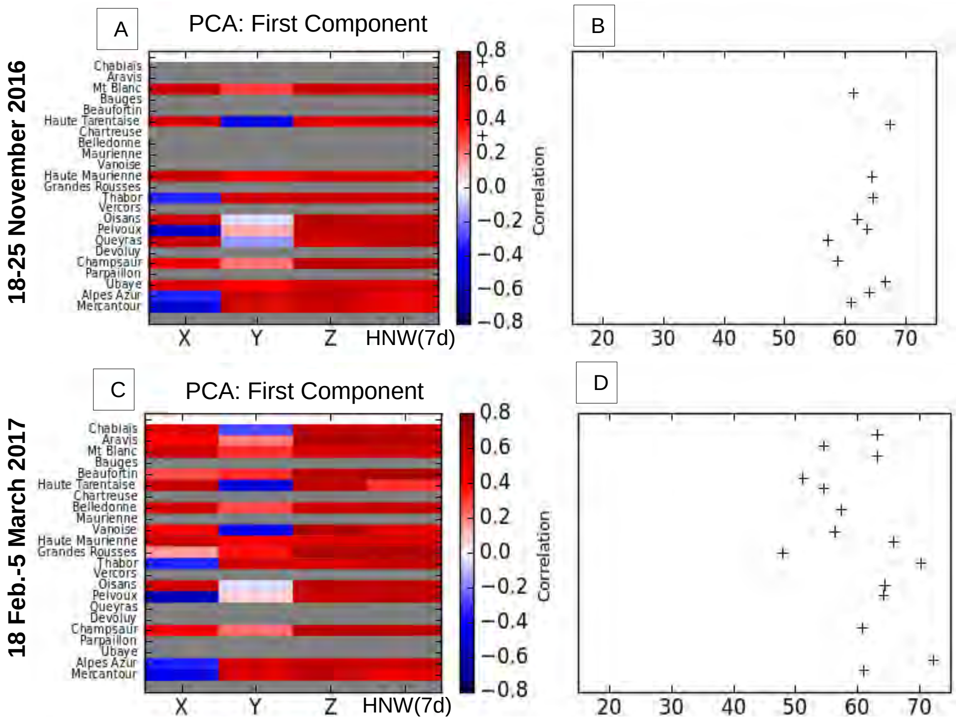

FIGURE 4.3: PCA results for the snowfall event A) from 18 November to 25 November 2016 and B) from the 28 February to the 5 March 2017. The grey colour indicates the non importance of this massif for this meteorological events.

altitude are strongly correlated to the component. The correlation of the longitude and latitude to the linear combination is variable regarding the event and the massif. For the first event (Fig. 4.3A) on the Queyras the longitude is positively correlated to the component with an important weight as the amount of new snow. Regarding Fig. 4.1 the amount of new snow is more important on the East side of the massif (where the longitude is the highest). These variables contribute to the linear combination with the same size as they evolve following the same direction.
For the second event on the Grandes-Rousses massif (Fig. 4.3C), the amount of new snow and the altitude are again strongly positively correlated to the component. The longitude is also slightly positively correlated to the component whereas the amount of snow is more important on the western part of the massif (Fig. 4.1D). As said above, the covariance matrix highlights a stronger correlation between the altitude and the longitude than in between the amount of new snow and the longitude. As the two covariance factors have opposed sign (respectively positive and negative), the PCA positively correlates the longitude to the component.

4.2 Spatial variability of stratigraphic profiles

In this section, the matching and clustering algorithms are applied to two variables describing the snowpack layering: Specific Surface Area (SSA) and density. The matching is applied on pairwise profiles to compute the distance between the profiles used to perform the clustering. Inside each cluster, the auto-matching method is performed to easily synthesise the data into a single representative profile including information of the variability of the cluster.

4.2.1 Case study

In this section the detailed method of the matching, clustering and auto-matching is illustrated by taking the example of the 5 March 2017 on the Queyras massif. The clustering is performed with 5 clusters. No snowpack properties will be discussed in this section since only the method is illustrated. The description of snowpack layering can be found on section 4.2.3.
The initial snow profiles are shown on Fig. 4.4A. For this date all profiles seems to be closed and so it is difficult to visually identify similar features inside each cluster. The matching algorithm is applied to compute the distance matrix between profiles to the clustering algorithm. This matrix is shown on Figure 4.4B. Its representation is sorted by clusters and shows the difference between each profiles. Very different profiles can not be grouped in the same cluster. The clustering results are shown on Figure 4.4C and 4.4D where the color of the profiles corresponds to its associated cluster. Using the auto-matching method, the intra-variability between the profiles of the same cluster is minimized to identify clear patterns (Fig. 4.4D). All data are combined to form a single trend with less variability at a given depth. The representative profile of a cluster is the mean of the profiles calculated between the profiles auto-matched in a same cluster. The spatial representation of the clusters highlights that the clustering identifies grid points which are connected or in the same band of altitude which is expected and realistic (Fig. 4.4C).
The distance matrix is however very complicated to read highlighting a set of data which is not homogeneous with no clear resemblance after the matching. The auto-matching inside each clusters is essential for the readability of the snowpack layering informations coming from AROME/Crocus.

4.2.2 Temporal evolution of the stratigraphic features and clusters

Area and period presentation

To evaluate and discuss the temporal evolution of the stratigraphic features, we choose to study the Queyras massif for the 25 November 2016, 19 December 2016 and the 20 December 2017. Queyras massif is situated at the border between France and Italy and so it is exposed to major East return events which occurred during this winter (Fig. 4.5). During winter 2016/2017, Queyras has been affected by several snowfall events. To apply our methods, we were interested in the East return event which occurred from 18 November to 25 November 2016. It is characterised by a high spatial variability of the snow cover in the Queyras massif with a gradient from West to East (Fig. 4.5A,C). After then, we observe for one month, an anti-cyclonic period without precipitation and with snowpack settling at all altitudes and potential melting at low altitude. During this period, the matching/clustering will be tested to study the evolution of the clusters for a long dry period. It stops on 19 December 2016 with snowfall occurring over the Queyras. Later in the season, the snowfall event between the end of February and the beginning of March is studied. Indeed this snowfall event is very different from the East return event as no clear snowfall patterns can be identified. The principal meteorological fluxes are going from the West side to the East side of the Alps globally.

Temporal evolution

The matching and clustering are applied for the simulation points presenting more than 30 cm of snow. The algorithms are computed at the end of the East return event (25 November 2016), after one month dry period (19 December 2016) and right after the snowfall event of the 20 December (Fig. 4.6). At the end of the East return event, huge quantities of fresh snow are identified for several profiles observed with high SSA around 50-60 m^2 kg^{-1}. The profiles with SSA around 25-30 m^2 kg^{-1} are also characterized of new fresh snow. Crocus accounts for the mechanical transformations of snow grains during snowfall observed in windy conditions (fragmentation). We observe

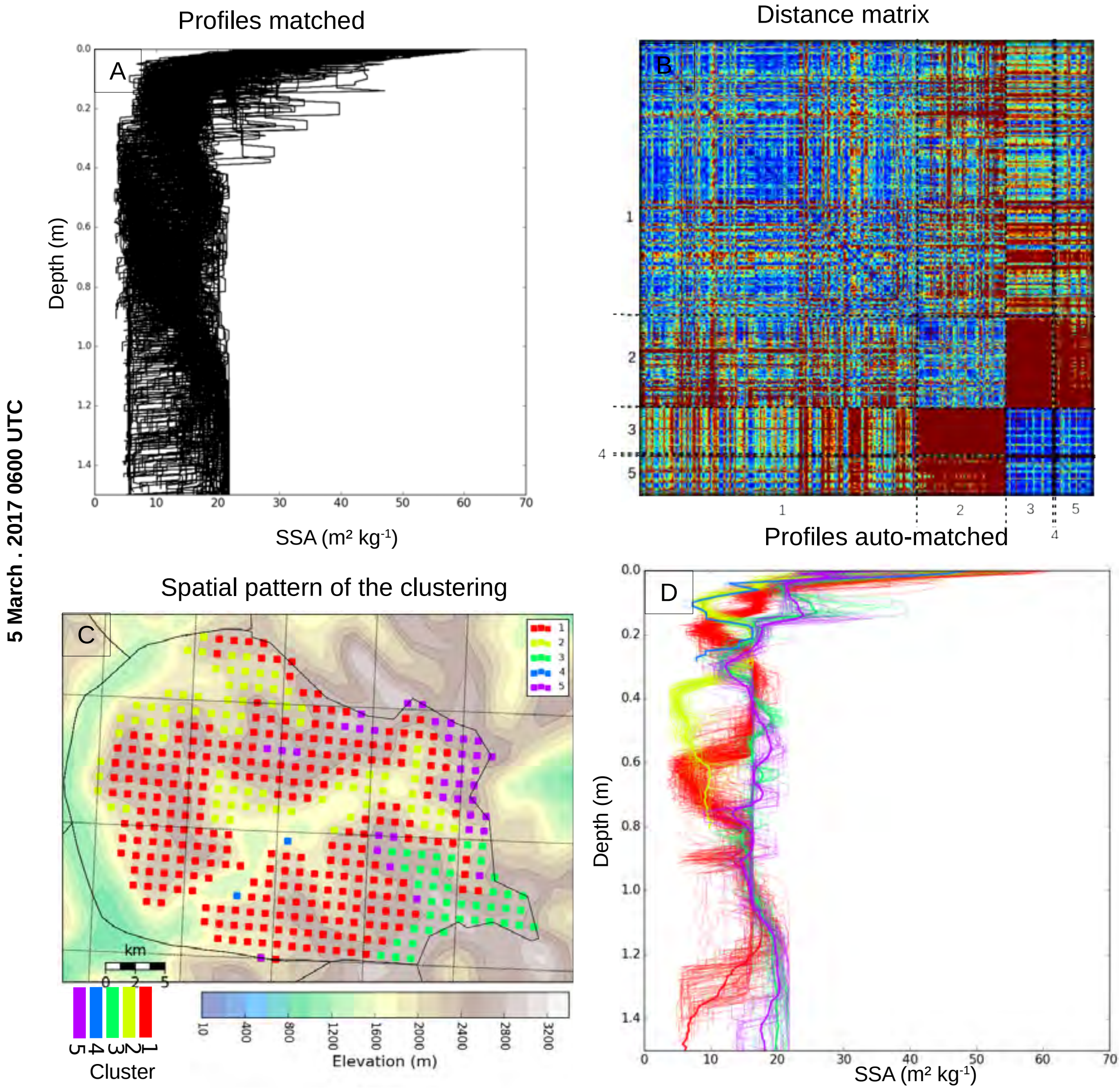

FIGURE 4.4: Clustering and matching applied on the 5 March 2017 on the Queyras massif based on the SSA. A) Initial profiles. B) The distance between each profiles is calculated to separate them into C) 5 clusters. D) The auto-matching algorithm is applied to perform representative profile of the cluster (thick line).

a high variability of the profiles even after the auto-matching. The variability of the altitude of the profiles on each cluster is also important (Fig. 4.6C). The cluster 1 groups the snow profiles of the low altitude and with a thinner snowpack. Clusters 2,3 and 4 group the pixels presenting all along the profile moderate to high values of SSA (between 25 and 65 m^2 kg^{-1}). Their spatial repartition (Fig. 4.6B) represent areas affected by the East return. The difference between these clusters comes from different wind speed during the snowfall event.
After a month without precipitation, the SSA value for all the profiles is between 10 and 20 m^2 kg^{-1} corresponding to a rounding of the grains with settling or melting processes as well as presence of moderate gradient benefiting the formation of angular grains. The clustering is made regarding the altitude on the 19 December 2016 (Fig. 4.6C) and they present a high vertical variability. For this event the maximum value of the SSA is 17 m^2 kg^{-1}. It corresponds to the maximal

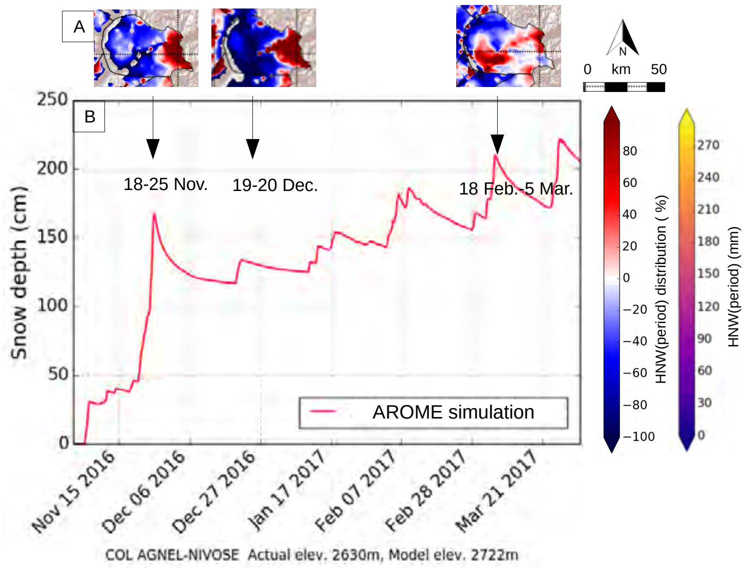

FIGURE 4.5: Snow cover situation in the Queyras for the winter 2016/2017. A) figures represent representative snowfall events in the $HNW(7d)$ detrended from altitude effect maps. In B) shows AROME simulations output concerning the snow depth at the Col Agnel (Fig. 2.1)during all from November 2016 to March 2017.

value of SSA parametrized in Crocus for faceted crystals. This threshold value means that the December dry cold period contributes to the transformation of snow crystals in faceted crystals at high altitude. It could also be crystals affected by melting processes. Despite the dry period, we retrieve the spatial distribution of the East return event occurring one month before (Fig. 4.6B), the cluster 1 representing the cluster 3 of the previous event. At low altitude layers can have been affected by melting processes. As profiles are superimposed we can not assure the present of a melting crust but only underlines this possibility.
The second snowfall of the season on 20 December 2016 deposits 20 cm of fresh snow for the highest part of the Queyras massif. On the snow profiles (Fig. 4.6A) the increase of the SSA up to 65 m^2 kg^{-1} witnesses this snowfall event. The cluster 1 and 3 highlights the presence of new snow with different characteristics. The cluster 1 has the highest SSA value and describes the snowfall occurring with low wind speed, mainly in the valley sheltered from the wind. On the contrary cluster 3 identifies windy area such as ridges at the East of the massif (Fig. 4.6B). The cluster 3 characterises areas affected by wind-induced snow transport and this information can be relevant for avalanche hazard forecasting. The underneath layers keep the footprint of the long dry period with several profiles of SSA at 17 m^2 kg^{-1}.
The study of the SSA provides relevant informations concerning the evolution of the snowpack over a snowfall event and over a long dry period. However this single information of SSA is not sufficient to determine the presence of weak layer in the snowpack essential for avalanche hazard forecasting.

4.2.3 Matching and clustering applied to different variables

The snowpack properties are defined by several variables which give different informations. Studying only the SSA is too poor to characterise snowpack layering at a given date. In this section, we will study the evolution of both SSA and density on 5 March 2017 at the end of snowfall event occurring from the 28 February 2016 (Fig. 4.7).

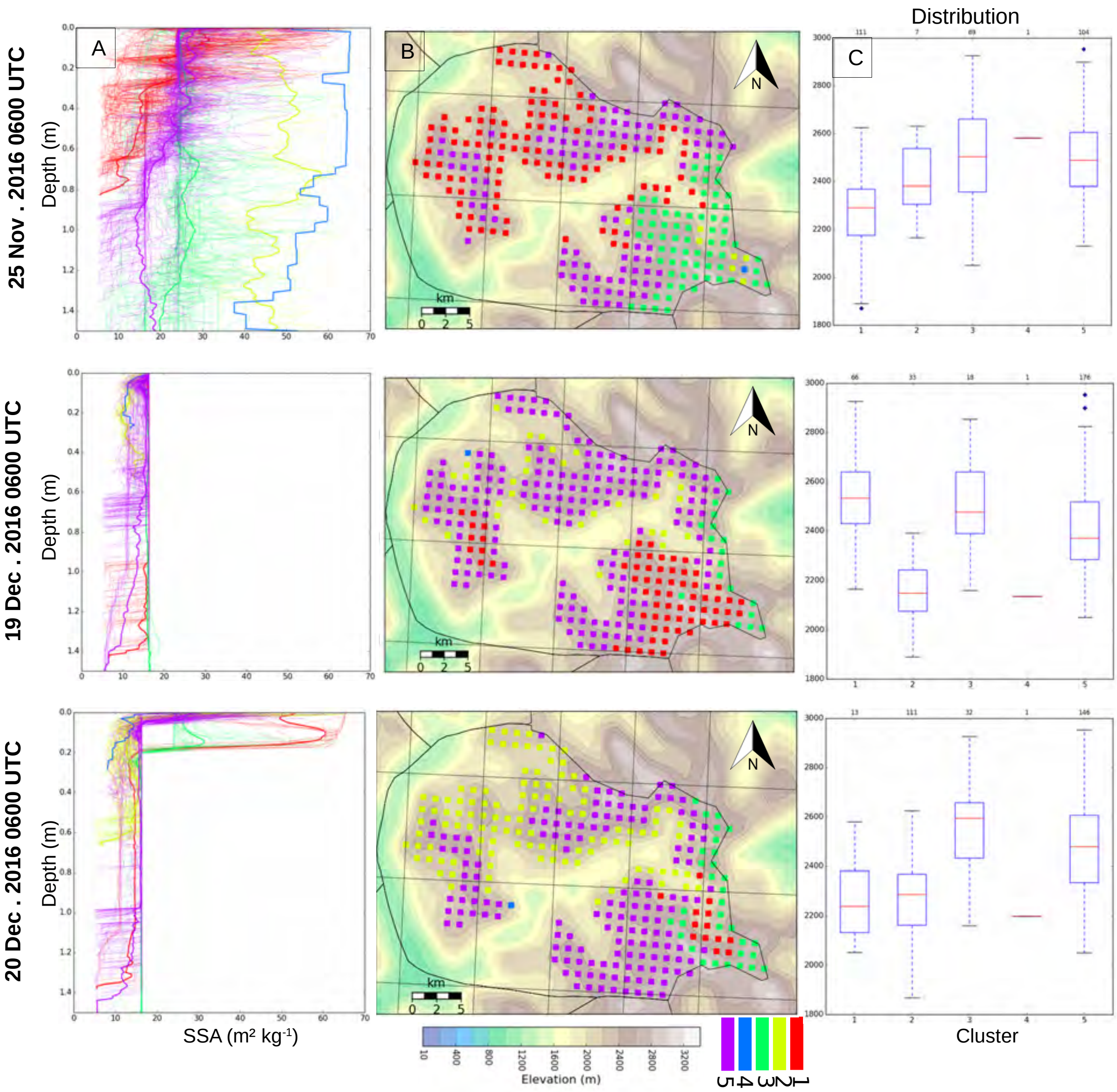

FIGURE 4.6: Matching and clustering on SSA on the 18 November 2016, 25 November 2016 and 19 December 2016. The figures A) presents the representative SSA profiles of each cluster (thick line) and the representative profiles for each cluster (thin line), B) the spatial repartition of the clusters and C) the distribution of the for each cluster.

Figure 4.7 shows the result of the matching/clustering on the 5 March 2016 for density and SSA (Fig. 4.7A, B). The first cluster is dominating the others grouping 62% of the pixels for the SSA and 61% for density. These pixels belong to the medium altitude range (median at 2300 m a.s.l.) but still have an important variability around the median. The spatial distribution of this cluster is similar for the two variables. The fresh snow at the surface snowpack is identified in the profiles with SSA values around 60 m^2 kg^{-1} and density values around 120 kg m^{-3}. A layer which has been affected by melting processes is also found in the both profiles at 20 cm under the surface (low SSA of 10 m^2 kg^{-1} and high density of 400 kg m^{-3}). A layer with similar characteristics is marked for SSA profiles at 60 cm below the surface whereas no increase of density is observed. The clustering performed on the SSA separates two clusters at the border with Italy whereas no

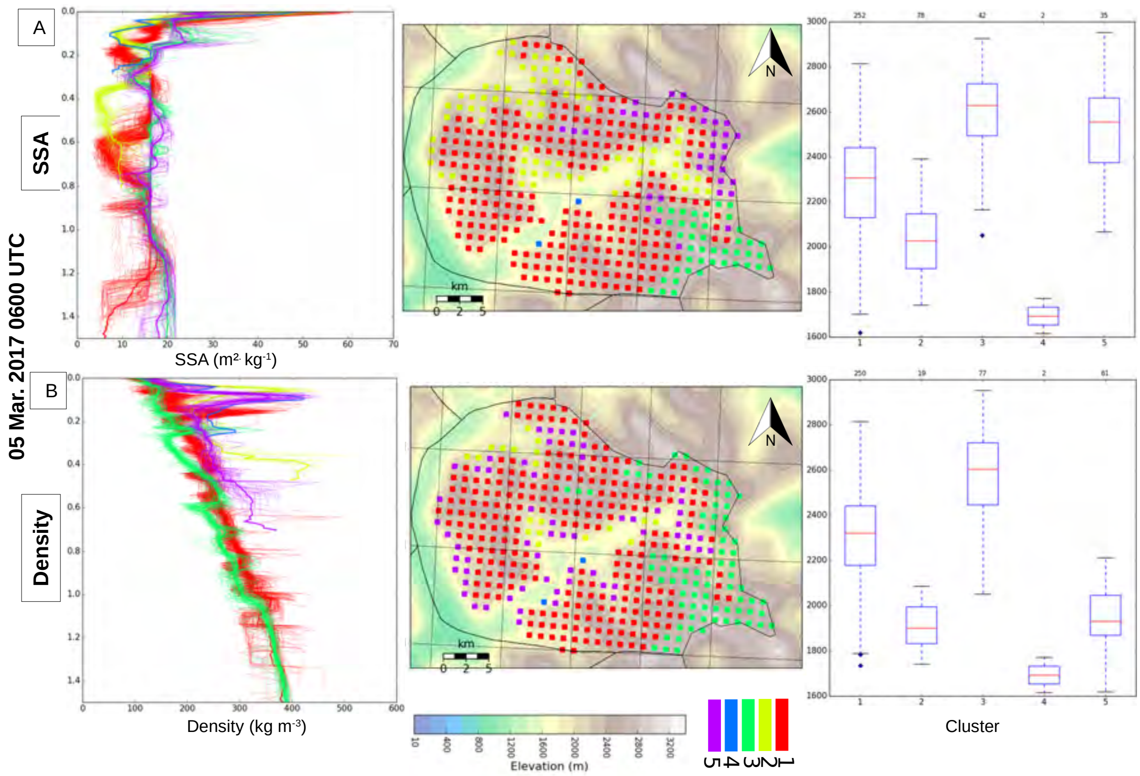

FIGURE 4.7: Matching and clustering of the density and the SSA for the 28 February 2016 and the 05 March 2016. The figures A) presents the representative density profiles of each cluster, B) the spatial repartition of the clusters and C) the distribution of the data set over each cluster.

differentiation is made for density. Regarding the SSA profiles, those two clusters (3 and 5) are however very close. The density profiles highlight a layer with low density (200 kg m^{-3}) at 60 cm from the surface which is not visible in the SSA profiles on this cluster.
Clusters 2 and 4 group pixels at low altitude (receptively the median is at 2300 m, 1700 m for SSA and 1900 m ,1700 m for density). The method differentiates them by the total height of snow.
The spatial locations of the cluster identified on SSA or density profiles slightly differ. These locations present a similar pattern at the Italian border. Inside the massif, the SSA-clusters do not show any clear specific pattern: only two clusters (5 and 3) cover this area. On the contrary, the density-clusters identify more significant groups in this area. This observation underlines the fact that combining several layer properties (e.g. density, SSA, hardness, sphericity) is necessary to capture the full variability of snowpack stratigraphy.

Chapter 5

Discussion and conclusion

Avalanche formation is partially controlled by the amount of new snow and the snowpack stratigraphy, especially in presence of weak layers. Following principal meteorological fluxes, the snow cover is not homogeneously distributed over the Alps. The quantification of this spatial variability is essential at the intra-massif scale for avalanche hazard forecasting. AROME high resolution system can be used to drive the snowpack model Crocus at kilometre scale over the French Alps. To use the variables simulated by AROME/Crocus for avalanche hazard forecasting, the development of synthesis tools is essential due to the huge quantity of data generated by these distributed snowpack simulations. In this study, the spatial variability of the amount of new snow is analysed by a simple approach and then the PCA is computed. The matching is coupled to the clustering method to synthesis the information of the snowpack properties. This study constitutes the first analysis of snowpack layering simulated by AROME/Crocus for the avalanche hazard forecasting. The analysis is made on the French Alps for winter 2016/2017.

$HNW(period)$ simulated by AROME/Crocus gives a first guess of the spatial patterns of snow accumulation resulting from a snowfall event. However the snow repartition is strongly linked to the terrain underneath. Thus, it is difficult to know whether a high amount of snow is due to a higher elevation or to a specific horizontal position in the massif. Removing elevation trend in the detrend of the $HNW(period)$ allows a better visualisation of the variability at the intra-massif scale. It enables to identify within a massif regions enhanced or reduced snow accumulation relative to local elevation. However the method has to be performed on a pre-defined geographical entity which constitutes a limitation for the characterisation of the spatial variability at the inter-massif scale. Using the actual geometry of the massif reveals discontinuity at the border of two massifs. The use of AROME is partly done to provide high resolution atmospheric forcing without pre-defined massif geometry implemented in SAFRAN reanalysis. The actual geometry of the massifs limits the comprehension of the spatial distribution of the snow at the inter-massifs scale. On Figure 5.1, $HNW(period)$ has been detrended from the altitude effect regarding other geometrical entities. At the entire Alps scale (Fig. 5.1C), the event highlights a major perturbation affecting the North-West of the Alps. For the event occurring in November (Fig. 5.1A and 5.1B) the border of Italy is marked by high amount of new snow regarding both scales. Large patterns of new snow distribution are identified on Fig. 5.1A. This scale allows to have an idea of the meteorological conditions occurring on the French Alps and the direction of the principal fluxes controlling the perturbation. However such a large scale is not relevant for avalanche hazard forecasting. The second experiment was performed using a moving circle with a radius equals to 17.23 km around each simulation points. The area of this circle is equals to the average size of the massifs in the French Alps. Snow distribution patterns appears and are not affected by discontinuities. This preliminary research highlights that the spatial variability of a snowfall depends on the scale. This tests illustrates this spatial variability.

To quantify the spatial variability at the intra-massif scale, the PCA has been performed for each massif of the domain for two snowfall events. The PCA was expected to partition the dependence of $HNW(period)$ on the altitude on one hand; on the other hand, the position within the

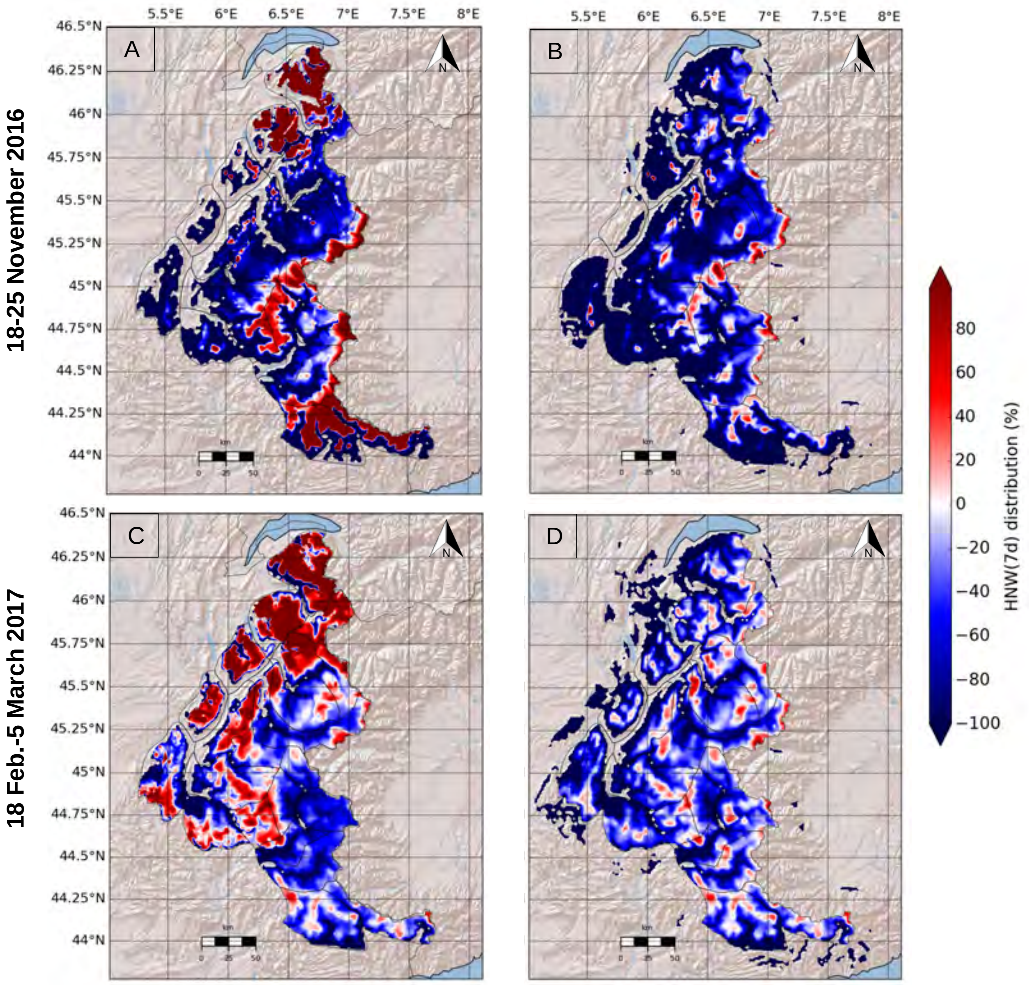

FIGURE 5.1: $HNW(7d)$ detrended from the altitude effect for different geographical entity. The detending method (Eq. 3.1) is applied use as a geographical entity the French Alps (A and C) or a circle corresponding to the typical size of a massif (radius: 17.2 km) around each pixel (B and D) The map is constructed with the simulated $HNW(7d)$ of the event from 18 to 25 Novembre 2016 and the one from 28 February and the 5 March 2017.

massif (characterized by the the longitude and the latitude). The first component of the PCA explains most of the variance up to 82% whereas the second component explains approximately 25% of the variance which is of the order of each original variable. The snowfall events is thus very simple to characterise because it can be done using a single linear combination of the original variables. The results of the PCA allows to quantify the strong positive and systematic dependence of $HNW(period)$ and the altitude to the first component. The horizontal distribution of the amount of new snow is understood and quantified thanks to the correlation factor of the longitude and latitude to the component. However the PCA would have been more successful in quantifying the spatial distribution of the amount of new snow if it had been performed regarding the snowfall events on each massifs. Correlation factor would have correlated massifs where snow accumulation exhibits similar patterns for given snowfall events.
The stratigraphy of the snowpack has been then studied to develop synthesis tool for avalanche hazard forecasting at the intra-massif scale. The simulated profiles comprises uncertainties in the evolution of variables along a snow profile in depth. These differences between two profiles can be interpreted as apparent spatial variability. The matching algorithm makes the distinction between

the variables variability and the depth variability. This algorithm coupled with the clustering is proposed as a practical method for combining data into synthetic information concerning snowpack layering. In this study the matching, clustering and auto-matching algorithms are applied to the density and SSA.

The matching algorithm is generic and can be applied to any kind of variables describing the snow profiles. The snow profiles can not be analysed without applying matching algorithm to overcome the apparent difference in depth of the layering of the snowpack. The spatial representation of the cluster is sorted regarding the altitude band or the connectivity of the pixels. The clusters are then realistic and underline the snow cover patterns highlighted with the maps of $HNW(period)$. Before the auto-matching algorithm is applied, differences between snow profiles are still hard to visualised. The auto-matching method is a relevant method for the computation of a representative profile of a cluster. It has limitation when high variability between each profiles is observed within a cluster. As the representative profile is computed taking the mean, the more the variability of the profiles is important the more the mean is flatten. This induces that major informations concerning snowpack properties are lost in the computation of representative profile.

To choose the number of cluster, sensitivity tests were performed to find the optimal representation of the snow cover patterns (Fig. 5.2). 3 clusters give not enough details of the spatial variability and appears to be very restrictive for an entire massif. With ten clusters no clear snow patterns are found and it makes the interpretation of the clustering confusing. 5 clusters appears to be the optimal number of cluster for our study as the configuration of Crocus is made with flat pixel. The actual method is not able to calculate the optimal number of cluster needed. This constitutes a limitation as this number should be variable and depends on the meteorological conditions. In this study this could explains the presence of mini-cluster grouping 1 or 2 pixels. This test could have been applied to 7 clusters for the comparison with SAFRAN analysis as its architecture has a vertical resolution of 300 m (in the Queyras the lowest pixels is at 1200 m a.s.l. and this highest at 3000 m a.s.l.). Python package scipy.cluster.hierarchy is able to defined the optimal number of cluster. The user needs to provide a maximal distance between cluster after which the merging of clusters is not significant.

The layering of the snowpack after matching, clustering and auto-matching allows to generate a

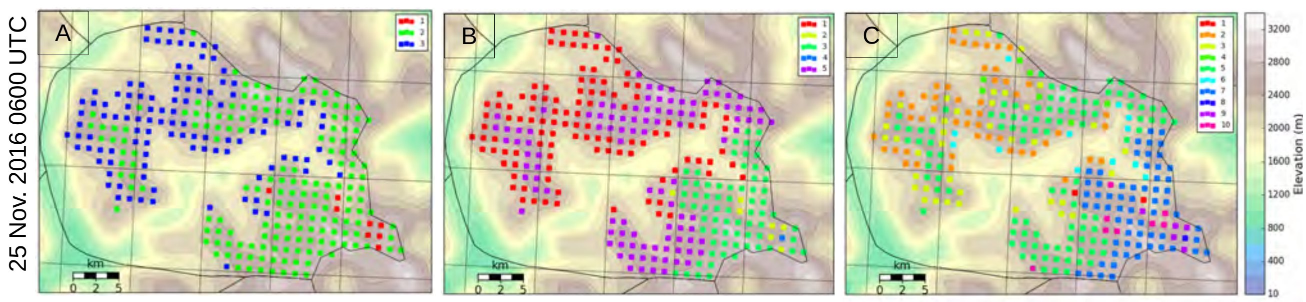

FIGURE 5.2: Sensitivity test for the choice of the cluster's number on the 25 November 2016. A) is clustering with 3 clusters, B) the clustering with 5 clusters and C) the clustering computed 10 clusters.

single representative profile per cluster. Using this method with a single variable can not succeed to achieve the entire characterisation of the snowpack properties relevant for avalanche hazard forecasting. Complementary variables (e.g. density, sphericity, hardness, age) should be analysed in the same time to analyse more precisely the snow cover layering (e.g. the grain type, the properties of a weak layers, its depth). As the matching is in this study computed separately for

different variables, analysis errors are easy to make because the matching of profiles of one variable can identify a weak layer at a different depth compared to an other variable representative profile. The multi-variables matching algorithm is in development. The representative profiles performed with several variables could be a robust tool for the forecaster as it do not have to interpret different variable profiles to find an indication of the stability of the snowpack. This algorithm asked for pre-defined weights to apply to each variables. This reflection is ongoing.
This study proposes relevant methods to synthesis the information of high resolution snowpack simulation generated with AROME/Crocus and shows encouraging performance. AROME atmospheric forcing are still associated with large uncertainties in alpine terrain with direct consequences on Crocus snowpack simulations. Progress are ongoing at the Snow Research Center to develop a distributed analysis system to improve the quality of the atmospheric forcing. It will be possible to apply the synthesis tools developed during this study as soon as the improved distributed snowpack simulations will be available. Another potential applications of these tools concern ensemble snowpack simulations(Vernay et al., 2015; Lafaysse et al., 2017). Distributed simulations accounting for wind-induced snow transport or the effects of slope and aspect on incoming solar radiation will also be tested. They will require to use additional clusters to capture the snowpack spatial variability generated by these processes.

Bibliography

Bartelt, P. and Lehning, M.: A physical SNOWPACK model for the Swiss avalanche warning: Part I: numerical model, Cold Reg. Sci. Technol., 35, 123–145, 2002.

Bellaire, S., Jamieson, J., and Fierz, C.: Forcing the snow-cover model SNOWPACK with forecasted weather data, Cryosphere, 5, 1115, 2011.

Bellaire, S., Jamieson, J., and Fierz, C.: Corrigendum to" Forcing the snow-cover model SNOWPACK with forecasted weather data" published in The Cryosphere, 5, 1115–1125, 2011, Cryosphere, 7, 511–513, 2013.

Bellaire, S., Katurji, M., Schulmann, T., and Hobman, A.: Towards a High-Resolution Operational Forecasting Tool for the Southern Alps-New Zealand, in: Proceedings of the International Snow Science Workshop, Banff, Canada, pp. 388–393, 2014.

Bolognesi, R., Buser, O., and Good, W.: Local avalanche forecasting in Switzerland: strategy and tools, a new approach, in: International Snow Science Workshop, pp. 463–472, 1994.

Brousseau, P., Seity, Y., Ricard, D., and Léger, J.: Improvement of the forecast of convective activity from the AROME-France system, Q. J. Roy. Meteor. Soc., 142, 2231–2243, 2016.

Brun, E., David, P., Sudul, M., and Brunot, G.: A numerical model to simulate snow-cover stratigraphy for operational avalanche forecasting, J. Glaciol., 38, 13–22, 1992.

Chow, F. K., De Wekker, S. F., and Snyder, B. J.: Mountain weather research and forecasting: recent progress and current challenges, Springer Science & Business Media, 2012.

Durand, Y., Brun, E., Merindol, L., Guyomarch, G., Lesaffre, B., and Martin, E.: A meteorological estimation of relevant parameters for snow models, Ann. Glaciol., 18, 65–71, 1993.

Durand, Y., Giraud, G., Laternser, M., Etchevers, P., Mérindol, L., and Lesaffre, B.: Reanalysis of 47 years of climate in the French Alps (1958–2005): climatology and trends for snow cover, J. Appl. Meteorol. Clim., 48, 2487–2512, 2009a.

Durand, Y., Laternser, M., Giraud, G., Etchevers, P., Lesaffre, B., and Mérindol, L.: Reanalysis of 44 yr of climate in the French Alps (1958–2002): methodology, model validation, climatology, and trends for air temperature and precipitation, J. Appl. Meteorol. Clim., 48, 429–449, 2009b.

Ekström, M., Jönsson, P., and Bärring, L.: Synoptic pressure patterns associated with major wind erosion events in southern Sweden (1973-1991), Clim. Res., 23, 51–66, 2002.

Erfani, A., Mailhot, J., Gravel, S., Desgagné, M., King, P., Sills, D., McLennan, N., Jacob, D., et al.: The high resolution limited area version of the global environmental multiscale model and its potential operational applications, in: 11th conference on mesoscale processes, American Meteorological Society, Albuquerque, NM, USA, 2005.

Esteban, P., Jones, P. D., Martín-Vide, J., and Mases, M.: Atmospheric circulation patterns related to heavy snowfall days in Andorra, Pyrenees, Int. J. Climatology, 25, 319–329, 2005.

Föhn, P., Stoffel, M., and Bartelt, P.: Formation and forecasting of large (catastrophic) new snow avalanches, in: Proceedings of the 2002 International Snow Science Workshop, vol. 29, pp. 141–148, 2002.

Gauer, P.: Blowing and drifting snow in alpine terrain: a physically-based numerical model and related field measurements, Ph.D. thesis, Swiss Federal Institue of Technology of Zurich, 1999.

Giard, D. and Bazile, E.: Implementation of a new assimilation scheme for soil and surface variables in a global NWP model, Mon. Weather Rev., 128, 997–1015, 2000.

Giraud, G.: MEPRA: an expert system for avalanche risk forecasting, ISSW Proc., Breckenridge, CO, Breckenridge, Colorado, USA, pp. 4–8, 1992.

Grünewald, T., Stötter, J., Pomeroy, J., Dadic, R., Baños, I. M., Marturià, J., Spross, M., Hopkinson, C., Burlando, P., and Lehning, M.: Statistical modelling of the snow depth distribution in open alpine terrain, Hydrol. Earth Syst. Sc., 17, 3005, 2013.

Grünewald, T., Bühler, Y., and Lehning, M.: Elevation dependency of mountain snow depth, Cryosphere, 8, 2381–2394, 2014.

Hagenmuller, P. and Pilloix, T.: A new method for comparing and matching snow profiles, application for profiles measured by penetrometers, Front. Earth Sci., 4, 52, 2016.

Hevesi, J. A., Istok, J. D., and Flint, A. L.: Precipitation estimation in mountainous terrain using multivariate geostatistics. Part I: structural analysis, J. Appl. Meteorol., 31, 661–676, 1992.
Horton, S., Schirmer, M., and Jamieson, B.: Meteorological, elevation, and slope effects on surface hoar formation, Cryosphere, 9, 1523–1533, 2015.
Hotelling, H.: Analysis of a complex of statistical variables into principal components., J. Educ. Psychol., 24, 417, 1933.
Kidson, J. W.: Relationship of New Zealand daily and monthly weather patterns to synoptic weather types, Int. J. Climatol., 14, 723–737, 1994.
Lafaysse, M., Morin, S., Coléou, C., Vernay, M., Serça, D., Besson, F., Willemet, J.-M., Giraud, G., Durand, Y., and Météo-France, D.: Towards a new chain of models for avalanche hazard forecasting in French mountain ranges, including low altitude mountains, in: Proceedings of International Snow Science Workshop Grenoble–Chamonix Mont-Blanc, pp. 162–166, 2013.
Lafaysse, M., Cluzet, B., Dumont, M., Lejeune, Y., Vionnet, V., and Morin, S.: Multiphysics ensemble-based modelling of an alpine snowpack, in: EGU General Assembly Conference Abstracts, vol. 19, p. 5230, 2017.
Lehning, M., Löwe, H., Ryser, M., and Raderschall, N.: Inhomogeneous precipitation distribution and snow transport in steep terrain, Water Resour. Res., 44, 2008.
Mailhot, J., Bélair, S., Lefaivre, L., Bilodeau, B., Desgagné, M., Girard, C., Glazer, A., Leduc, A.-M., Méthot, A., Patoine, A., et al.: The 15-km version of the Canadian regional forecast system, Atmos. Ocean, 44, 133–149, 2006.
Masson, V., Le Moigne, P., Martin, E., Faroux, S., Alias, A., Alkama, R., Belamari, S., Barbu, A., Boone, A., Bouyssel, F., et al.: The SURFEXv7. 2 land and ocean surface platform for coupled or offline simulation of earth surface variables and fluxes, Geosci. Model Dev., 6, 929–960, 2013.
McClung, D. and Schweizer, J.: Skier triggering, snow temperatures and the stability index for dry-slab avalanche initiation, J. Glaciol., 45, 190–200, 1999.
Mott, R., Schirmer, M., Bavay, M., Grünewald, T., and Lehning, M.: Understanding snow-transport processes shaping the mountain snow-cover, Cryosphere, 4, 545, 2010.
Mott, R., Scipion, D., Schneebeli, M., Dawes, N., Berne, A., and Lehning, M.: Orographic effects on snow deposition patterns in mountainous terrain, J. Geophys. Res. Atmos., 119, 1419–1439, 2014.
Pearson, K.: LIII. On lines and planes of closest fit to systems of points in space, The London, Edinburgh, and Dublin Philosophical Magazine and Journal of Science, 2, 559–572, 1901.
Petitjean, F., Ketterlin, A., and Gançarski, P.: A global averaging method for dynamic time warping, with applications to clustering, Comm. Com. Inf. Sc., 44, 678–693, 2011.
Pomeroy, J. and Gray, D.: Snowcover accumulation, relocation and management, B. Int. Soc. Soil Sci. no, 88, 1995.
Quéno, L., Vionnet, V., Dombrowski-Etchevers, I., Lafaysse, M., Dumont, M., and Karbou, F.: Snowpack modelling in the Pyrenees driven by kilometric-resolution meteorological forecasts, Cryosphere, 10, 1571–1589, 2016.
Romero, R., Ramis, C., and Guijarro, J.: Daily rainfall patterns in the Spanish Mediterranean area: an objective classification, Int. J. Clim., 19, 95–112, 1999.
Rousselot, M., Durand, Y., Giraud, G., Merindol, L., and Daniel, L.: Analysis and forecast of extreme new-snow avalanches: a numerical study of the avalanche cycles of February 1999 in France, J. Glacio., 56, 758–770, 2010.
Sakoe, H. and Chiba, S.: Dynamic programming algorithm optimization for spoken word recognition, IEEE transactions on acoustics, speech, and signal processing, 26, 43–49, 1978.
Schweizer, J.: The influence of the layered character of snow cover on the triggering of slab avalanches, Ann. Glaciol., 18, 193–198, 1993.
Schweizer, J., Jamieson, J. B., and Skjonsberg, D.: Avalanche forecasting for transportation corridor and backcountry in Glacier National Park (BC, Canada), 25 Years of Snow Avalanche Research, Voss, Norway, 12-16 May 1998, pp. 238–243, 1998.
Schweizer, J., Bruce Jamieson, J., and Schneebeli, M.: Snow avalanche formation, Rev. Geophys., 41, 2003.
Schweizer, M., Föhn, P., Schweizer, J., and Ultsch, A.: A hybrid expert system for avalanche forecasting, in: Information and Communications Technologies in Tourism, pp. 148–153, Springer, 1994.
Seity, Y., Brousseau, P., Malardel, S., Hello, G., Bénard, P., Bouttier, F., Lac, C., and Masson, V.: The AROME-France convective-scale operational model, Mon. Weather Rev., 139, 976–991, 2011.

Silverman, N. L., Maneta, M. P., Chen, S.-H., and Harper, J. T.: Dynamically downscaled winter precipitation over complex terrain of the Central Rockies of Western Montana, USA, Water Resour. Res., 49, 458–470, 2013.

Vernay, M., Lafaysse, M., Mérindol, L., Giraud, G., and Morin, S.: Ensemble forecasting of snowpack conditions and avalanche hazard, Cold Reg. Sci. Technology, 120, 251–262, 2015.

Vionnet, V., Brun, E., Morin, S., Boone, A., Faroux, S., Le Moigne, P., Martin, E., and Willemet, J.: The detailed snowpack scheme Crocus and its implementation in SURFEX v7. 2, Geosci. Model Dev., 5, 773–791, 2012.

Vionnet, V., Martin, E., Masson, V., Guyomarc'h, G., Bouvet, F. N., Prokop, A., Durand, Y., and Lac, C.: Simulation of wind-induced snow transport and sublimation in alpine terrain using a fully coupled snowpack/atmosphere model, Cryosphere, 8, p–395, 2014.

Vionnet, V., Dombrowski-Etchevers, I., Lafaysse, M., Quéno, L., Seity, Y., and Bazile, E.: Numerical weather forecasts at kilometer scale in the French Alps: evaluation and application for snowpack modeling, J. Hydrometeorol., 17, 2591–2614, 2016.

Xue, M., Droegemeier, K. K., and Wong, V.: The Advanced Regional Prediction System (ARPS)–A multiscale nonhydrostatic atmospheric simulation and prediction model. Part I: Model dynamics and verification, Meteorol. Atmos. Phys., 75, 161–193, 2000.

Appendix A

Comparaison of AROME 1.3km with SAFRAN reanalysis

In this section we take as an example two very different meteorological events in order to compare AROME 1.3 km compared to SAFRAN.

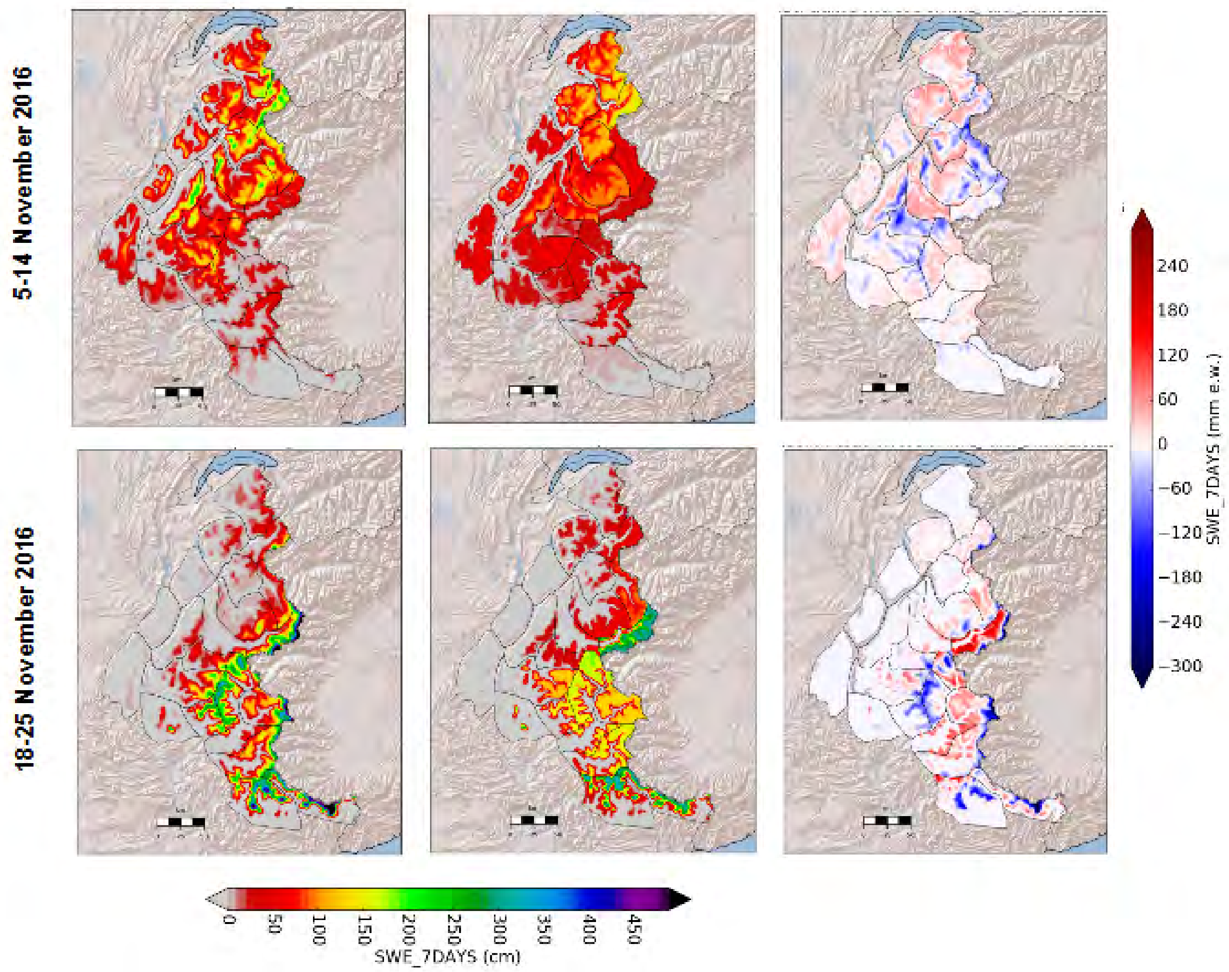

FIGURE A.1: Maps of snowfall (SWE w.e.) for two different meteorological event described in Chapter 2. The first column gives the simulated snow cover by AROME/Crocus. The second column gives the simulated snow cover by SAFRAN reanalysis and the third column the difference between SAFRAN and AROME snow cover.

Figure A.1 shows the simulated Snow Water Equivalent (SWE in mm w.e.) over the French

Alps for the two first events of the season 2016/2017 described in Chapter 2. The variable used in the SWE cumulated over 7 days. Both models simulated well the spatial distribution of the snow cover across the Alps during this two events. It shows the influence of the underlying topography.The maximum of the precipitation are in the same massif, for the first event, located in the Mont Blanc mountain range and for the second event on the massif in the border of Italy (e.g. HAute Maurienne, Queyras, Mercantour). However their are large differences at the border of Italy btween the two models. SAFRAN is for all massifs in this area in deficit of snow. On the second event the is more snow in AROME than in SAFRAN for the upwind side (west) and we observe the opposite for the downwind side (East).
It is clear on the map that SAFRAN do its reanalysis on a massif without taking into account the other pixels on the other massif. Their are cleavages between the snow cover in one massif and its neighbour. This characteristic is clearly observed on the second event (Figure A.1-bottom,middle) between Mercantour and Ubaye or between Thabor and Grande Rousse. AROME which runs on a grid does not show this patterns. Their is continuity between each massif.